

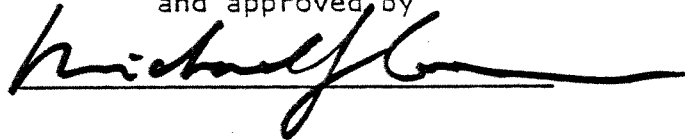
AN INVESTIGATION OF THE EFFECTS OF THE SOLID EARTH
TIDES ON THE TRIGGERING OF VOLCANIC ERUPTIONS
IN CENTRAL AMERICA

by JEFFREY E. GOLDENBERG

A thesis submitted to
the Graduate School
of
Rutgers University
in partial fulfillment of the requirements
for the degree of
Master of Science

Written under the direction of
Professor Michael J. Carr
of the Department of Geology

and approved by

A handwritten signature in black ink, appearing to read "Michael J. Carr", is written over a horizontal line. Below this line are two more horizontal lines, which are currently blank.

New Brunswick, New Jersey

May, 1978

ABSTRACT OF THE THESIS

An Investigation of the Effects of the Solid Earth Tides on the Triggering of Volcanic Eruptions in Central America

by JEFFREY E. GOLDENBERG

Thesis director: Professor Michael J. Carr

Triggering of volcanic eruptions has been linked to the solid earth tides. If this correlation is valid, onset of eruptions should occur when accelerations of gravity reach maximum amplitudes. A computer program supplied by Henry Pollack (personal communication) was used to derive various earth tidal data. The times for initial eruptions of volcanoes in Central America were compared with these data and no statistical correlation was found.

ACKNOWLEDGEMENTS

Special thanks are extended to the following individuals, whose assistance and constant enthusiasm allowed this study to succeed: Dr. Michael Carr, for constant guidance through every stage and for his time and effort in designing the project and critical reviews of the manuscript; Dr. Martha Hamil for her critical review of the manuscript and encouragement at the beginning of my geologic career; Dr. Steven Fox for his critical review of the manuscript and his fantastic ability to stirr the imagination and make studying geology a true pleasure; and Darryl Mayfield for his assistance in many ways.

This thesis was supported by the Division of Earth Sciences, National Science Foundation, under grant EAR 76-09377.

TABLE OF CONTENTS

Title-Page	i
Abstract	ii
Acknowledgements	iii
List of Figures	v
Introduction	1
Previous Work	1
Geologic Setting	2
Earth Tides	2
Eruption Data	6
Method	6
Eruption Characterization	6
Description of Tidal Cycles Examined	6
Preparation of Histograms	8
Statistical Method	9
Synoptic and Monthly Analysis	10
Results	10
Full Cycle	10
Reduced Cycle	23
Effects of Segments	31
Synoptic and Monthly Analysis	33
Conclusion	36
Appendix I	37
Appendix II	48
References	60

LIST OF FIGURES

<u>Number</u>	<u>Description</u>	<u>Page</u>
1	Index Map	3
2	Vector Component Plot	4
3	Total Vector	11-13
4	North-South	14-16
5	Synodic	17-19
6	Anomalistic	20-21
7	Reduced Cycles	24-26
8	Total Eruptions- Total Vector	27
9	Total Eruptions- North-South	28
10	Total Eruptions- Synodic	29
11	Total Eruptions- Anomalistic	30
12	Total Eruptions- Sum of Eruptions per segment	32
13	Synodic vs. Anomalistic	34
14	Total Eruptions- Calender Month	35

INTRODUCTION

The solid earth tides may trigger some volcanic eruptions. Semi-diurnal, diurnal, and 14.7 day tidal cycles constitute the largest short term oscillatory stresses in the earth's crust (Knopoff, 1964). Klein (1976), Mauk and Kienle (1973), Tamrazyan (1968) and others have suggested that tidal stresses in many places may be responsible for earthquake triggering. There has been less success, however, in relating major earthquakes to the solid earth tides. Solid earth tides are either demidiurnal, diurnal or mixed depending of the declination of the moon. The semi-monthly tidal effect is caused by the orbit of the moon and sun in relation to the earth.

The purpose of this thesis is to analyze the frequency of initial volcanic eruption times in terms of the cycles of the lunar month. The large number of historic volcanic eruptions in Central America make it a very attractive area for study.

PREVIOUS WORK

Mauk and Kienle (1973) found a relation between the semi-diurnal solid earth tides and peak microearthquake activity at St. Augustine Volcano, Alaska. Ryall, Van Wormer and Jones (1968) showed a correlation of the major aftershocks associated with a microearthquake swarm near Truckee, California in 1966 and the solid earth tidal record. Tamrazyan (1968) suggested the association of cosmic alignments and earthquake triggering in Norway. Knopoff (1964) studied a sample of earthquakes from southern California and indicated a linking with the tidal potential that is no greater than random. Morgan, Stoner, and Dicke (1961) analyzed 1,933 earthquakes for periodicity and presented no evidence for effects due to earth tides. Simpson (1967) compared the actual distribution and theoretical random distribution of 22,561

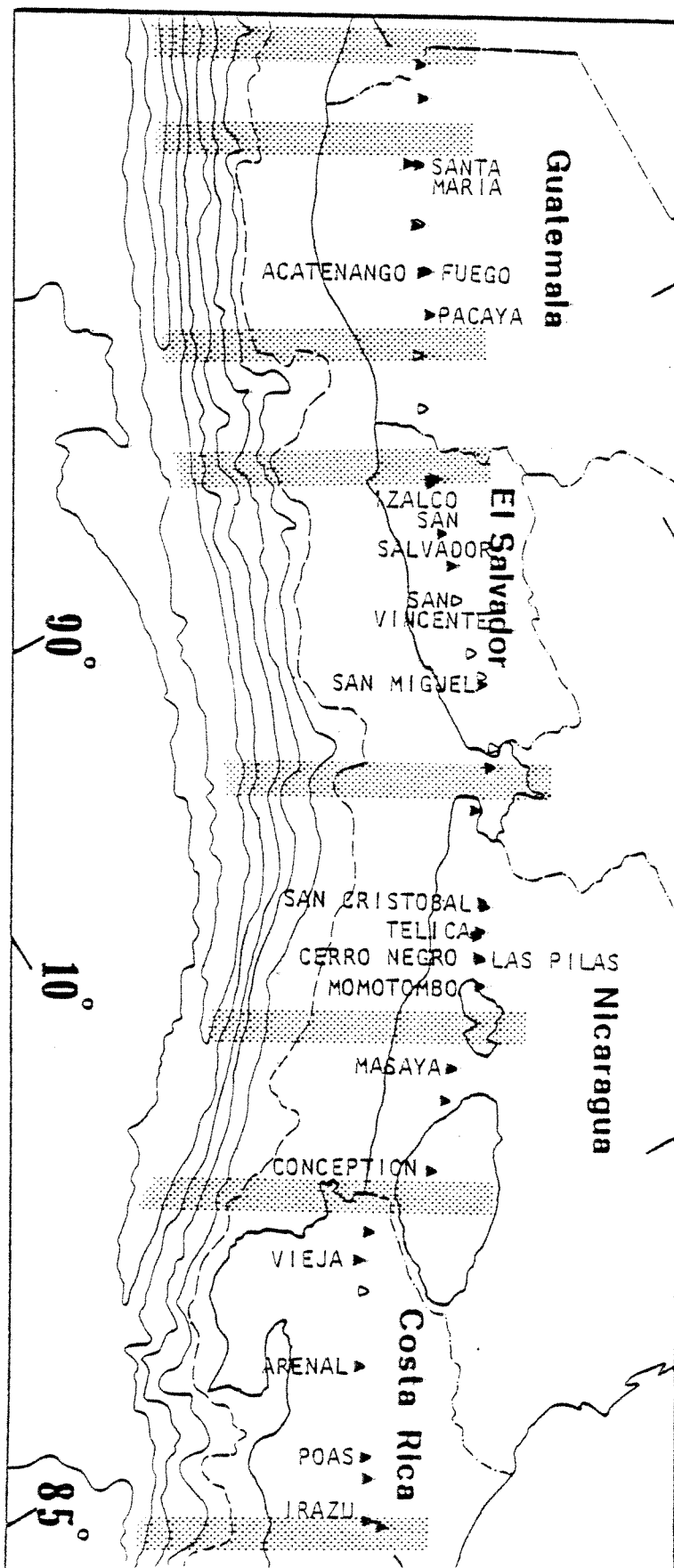
earthquakes and concluded that they are not triggered by accelerations of earth tide component forces. Mauk and Johnson (1973) catalogued the initial eruption times of 680 volcanoes and found that the probability of eruptions was greatest at times of maximum tidal amplitude. Hamilton (1972) noted favorable correlations in tidal triggering of volcanic eruptions when tidal amplitudes are largest at the latitude of the volcano.

GEOLOGIC SETTING

In Central America a chain of active volcanoes is located approximately 40 kilometers inland from the coast. The chain strikes northwest; parallel to both the Pacific coastline and the Middle America Trench. Earthquakes are concentrated in two zones. The first is an inclined zone that begins at the trench and dips from 30 to 60 degrees northeastward. The second is beneath the Central American volcanic belt (Molnar and Sykes, 1969; Stoiber and Carr, 1973). Stoiber and Carr (1973) have concluded that Central America is divided into seven segments, or discrete units. Evidence is based on the differences in strikes, positions, and morphology of volcanic lineaments in the historically active chain. The boundaries are limited by some discontinuities in the deep seismic zone, the distribution and concentration of shallow earthquakes, and by catastrophic eruptions. Faulting occurs transverse to the volcanic lineaments at these breaks as well. These segments, 100 to 300 kilometers in length, are assumed to be structural sub-units. The volcanoes studied are shown in Fig. 1. The segments are marked by broad stippled zones.

EARTH TIDES

Maximum peak to peak strain on the order of $\frac{1}{2} \times 10^{-7}$ occur bi-monthly with the full and new moon (Knopoff, 1964). This periodic

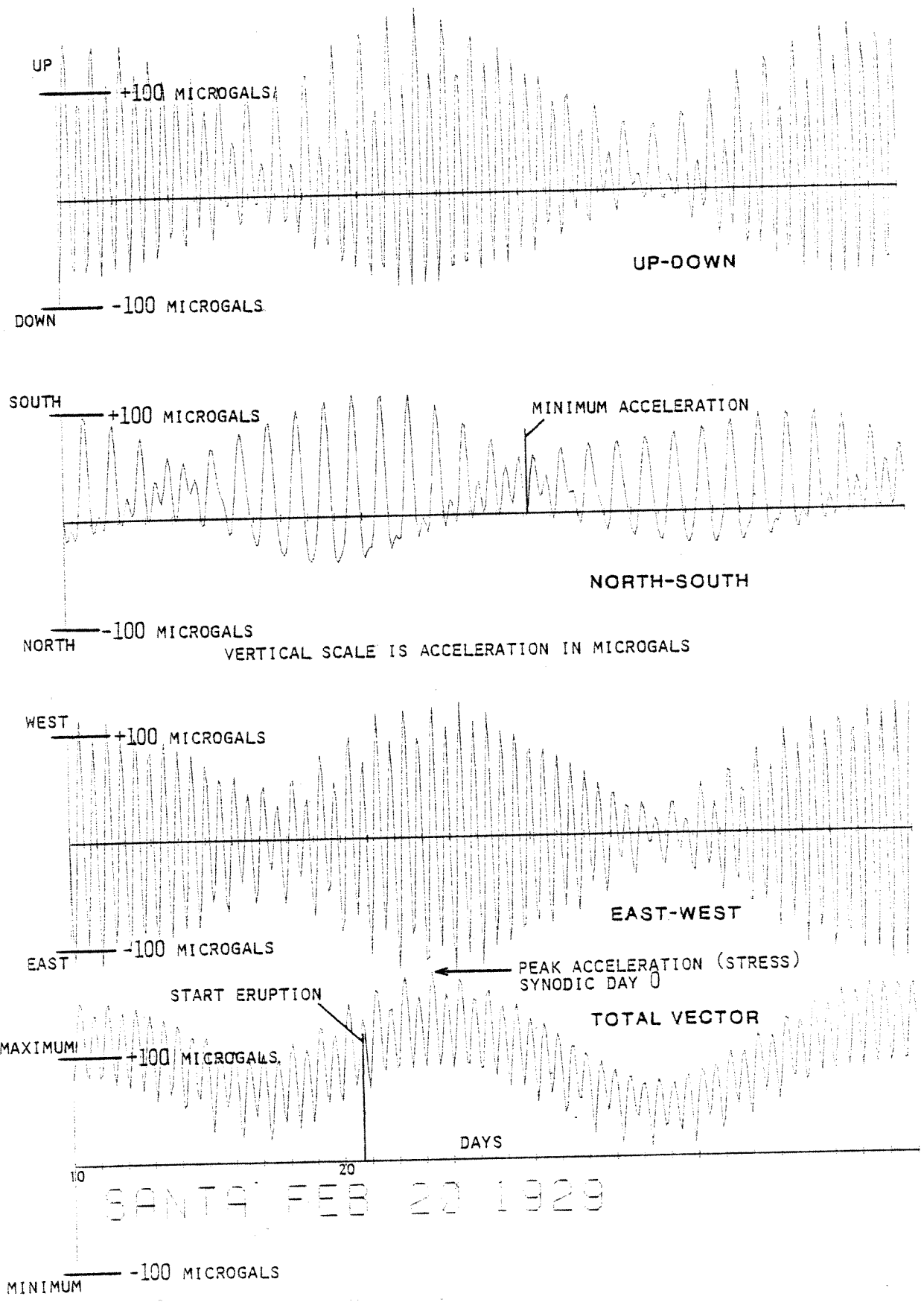


INDEX MAP

AFTER STOTTER AND CARR, 1973

OPEN TRIANGLES ARE HISTORICALLY ACTIVE VOLCANOES
CLOSED TRIANGLES ARE VOLCANOES WITH ONLY SOLTAFARA ACTIVITY

FIGURE 1



VECTOR COMPONENT PLOT

FIGURE 2

juxtaposition of sun and moon is called the synodic tidal cycle. The other components of the earth tides are the distances between the sun and the moon, namely the anomalistic cycle, and of secondary importance, the tropical cycle, which is the angle from the equator that the moon describes. The synodic cycle is about 29.5 days and the anomalistic or perigee-apogee cycle and tropical cycles are 27.5 days.

Vector components of the gravitational attraction of sun and moon add up to the total vector (Fig. 2). This vector is arbitrarily resolved into 3 components; the east-west, north-south, and vertical. The periodicity and intensity of the total vector closely follow the synodic cycle. The east-west and vertical components are the major influences of this similarity; the north-south function is almost always out of phase and is of variable duration, ranging from 13 to 16 days for periods measured between acceleration amplitude minima.

The synodic and anomalistic months and their components can be derived from equations of Longman (1964) and Pollack (1973). A computer program supplied by Pollack (personal communication) calculates the position of the sun and moon using astronomical equations and computes the acceleration of gravity at a point on the earth's surface. Pollack (1973) and Mauk and Johnson (1973) used this program and found that their calculations agree with published tidal observations from quartz strain meters and gravimeters. Garlands (1971) shows that maximum gravitational attractions are on the order of .3 milligals per meter. This is in accord with the accepted value of maximum peak to peak strain of $\frac{1}{2} \times 10^{-7}$ noted by Knopoff (1964). I have found acceleration amplitudes of up to 200 microgals which can account for total crustal deformation of .67 meters across the diameter of the earth. The value of $\frac{1}{2} \times 10^{-7}$ maximum strain can be converted to a value of .639 meters using 8,000 miles

as the earth's diameter.

ERUPTION DATA

Historic eruption dates are listed in the Appendices and were compiled from the Catalog of Active Volcanoes of the World, Bulletin Vulcanologique, Smithsonian Institution's Center for Short-Lived Phenomena Reports, field notes, and personal communications.

Volcanic eruption intensity ratings were assigned after comparison of descriptions of types of eruptions. Considerations of the most importance were judged by the size and distance of ash and bombs ejected, the distance, duration, and amount of ash fall, distance and intensity of SO_2 emitted, and amount of lava discharged. Nuee ardentes, smoke, and ash clouds as well as the extent of destruction of land and the loss of life were noted (Appendix II)

METHOD

Eruption Characterization

I have examined possible correlations of earth tides and times of the beginning of eruptions in Central America in order to test the hypothesis that volcanoes begin to erupt at a particular phase of the fortnightly cycle of the solid earth tides.

Description of Tidal Cycles Examined

The total vector function incorporates all aspects of the positions of the sun and moon relative to the earth; it adds the effects of gravitational attraction in 3 dimensions. The east-west and vertical components are very similar in amplitude and period to the total vector function.

The north-south component measures acceleration amplitudes in a north-south direction. The form of its cycle (shown in Fig. 2) is very different than the total vector function to which it contributes, how-

ever it also includes all aspects of the relative positions of the sun and moon.

The synodic tidal cycle is determined by the position of the moon and sun relative to the earth. Maximum gravitational attraction occurs when the angle measured from the earth to the sun and moon is zero or 180 degrees (new and full moon respectively). The weakest gravitational attraction occurs when the sun and moon describe a 90 degree angle from the earth (quarter moon). New and full moon are called the spring tides and quarter moon phases are the neap tides.

Histograms of the number of beginnings of eruptions versus the days of the tidal cycles are arranged in the order of the cycles described above. This order was determined by the value of information each cycle provided. The total vector function and north-south component were more valuable than the synodic cycle because all aspects of sun and moon positions were included and an accurate representation of their cycles could be plotted. The anomalistic cycle was least valuable since it was dependent only upon distance and not relative position.

Lunar cycles (synodic and anomalistic) and the total vector function and its north-south component were correlated to initial eruption times. Since the east-west and vertical components of the total vector function were so similar in periodicity and amplitude; they were difficult to work with. Semidiurnal and diurnal correlations were not attempted because most eruptions could not be verified to have begun at a specific hour of the day.

The time interval considered ranged from 1900 to the present. For simplicity, all data and figures were arranged in order of latitude from south to north. In addition, plate segments (Stoiber and Carr, 1973) are defined by dashed lines throughout the histograms of Figures 3

through 7.

Preparation of Eruption Frequency Histograms

Preparation of the histograms was dependent on the length of the individual cycles. Day zero for the synodic and total vector plots begins when the amplitude of acceleration reaches its highest value. Both the synodic and total vector cycles are approximately $29\frac{1}{2}$ days in duration, and since in most cases eruption times are not accurate to within more than one day, the cycles have been set at 30 days. The anomalistic month is 28 days; day zero begins at apogee. The north-south cycle averages 14 days and is measured from the nearest low amplitude acceleration.

The total vector and north-south histograms were derived from acceleration information supplied by a computer plotting routine. Days of eruptions were measured directly from the plot (Fig. 2). The synodic and anomalistic histograms were derived by interpolation of angular and distance values given in the printout. These data are summarized in Appendix I.

Figures 3a through 3c are plots of the frequency of eruptions during the total vector cycle for each Central American volcano. Day zero begins at the nearest day zero on the synodic cycle (highest gravitational acceleration). Figures 4a through 4c represent the frequencies and eruptions during the cycle of the north-south component. Day zero begins at maximum north-south gravitational acceleration. Figures 5a through 5c show the relation of eruptions to the synodic tidal cycle. Figures 6a through 6c show the relation of eruptions to the anomalistic cycle.

All cycles have shorter periods which can be plotted (see Figs. 7a through 7c). The synodic and total vector histograms can be broken down

into 15 day periods each; day 0 adds to day 15, day 1 adds to day 16, etc. This procedure is valid because added days represent very similar tidal accelerations. The anomalistic month can be represented by a 15 day cycle and the north-south component can be reduced to an 8 day cycle. There is nearly a mirror image in acceleration amplitudes centered at perigee so that adding days symmetrically outward toward apogee will validly shorten the anomalistic cycle and facilitate interpretation. The north-south cycle adds outward from minimum acceleration to maximum amplitude acceleration.

Figures 8 through 11 are summations of all eruptions plotted on the total vector, north-south, synodic, and anomalistic cycles. Additional histograms of these figures reduce the cycles and provide full and half cycle plots of all eruptions minus the data for Santa Maria due to the possible masking effect of an overbalance of historic eruptions from this frequently erupting volcano. When analyzing the peaks of reduced cycles of the north-south and anomalistic histograms, one must remember that since the center points are the pivots from which days are added, they themselves have no days to add. Therefore, their values are necessarily higher than indicated. The range of these specific days will be discussed in the results section. Figure 12 sums the eruptions for all volcanoes on the total vector plot and separates them by plate segments.

Statistical Method

Following the analysis of Klein (1976), the expected mean and standard deviations of eruptions for days of the tidal cycles were calculated with standard formulae for the binomial probability distribution ($m=np$ and $s.d.=np(1-np)$). If the number of events per day is random, one would expect them to cluster around the mean and be distributed within $\pm 2\sigma$ from

the mean. The number of events in a cycle is n , and p is the probability that one event will occur in a particular day (e.g., $1/14$ for a 14 day cycle).

Synoptic and Monthly Analysis

Figure 13 is designed after the synoptic diagram of Tamrazyan (1968) and Hamilton (1972). Maximum stress generation occurs when tidal cycles were in phase or 180 degrees out of phase with each other. Figure 13 relates initial eruption times with the synodic and the anomalistic lunar months. The diagonal lines mark approximate limits of 7 day periods in which lunar cycles are in phase and out of phase with each other.

In Figure 14, all historic eruptions are grouped by occurrence in the same calendar month in an attempt to see if there is any seasonal effect on eruption frequency.

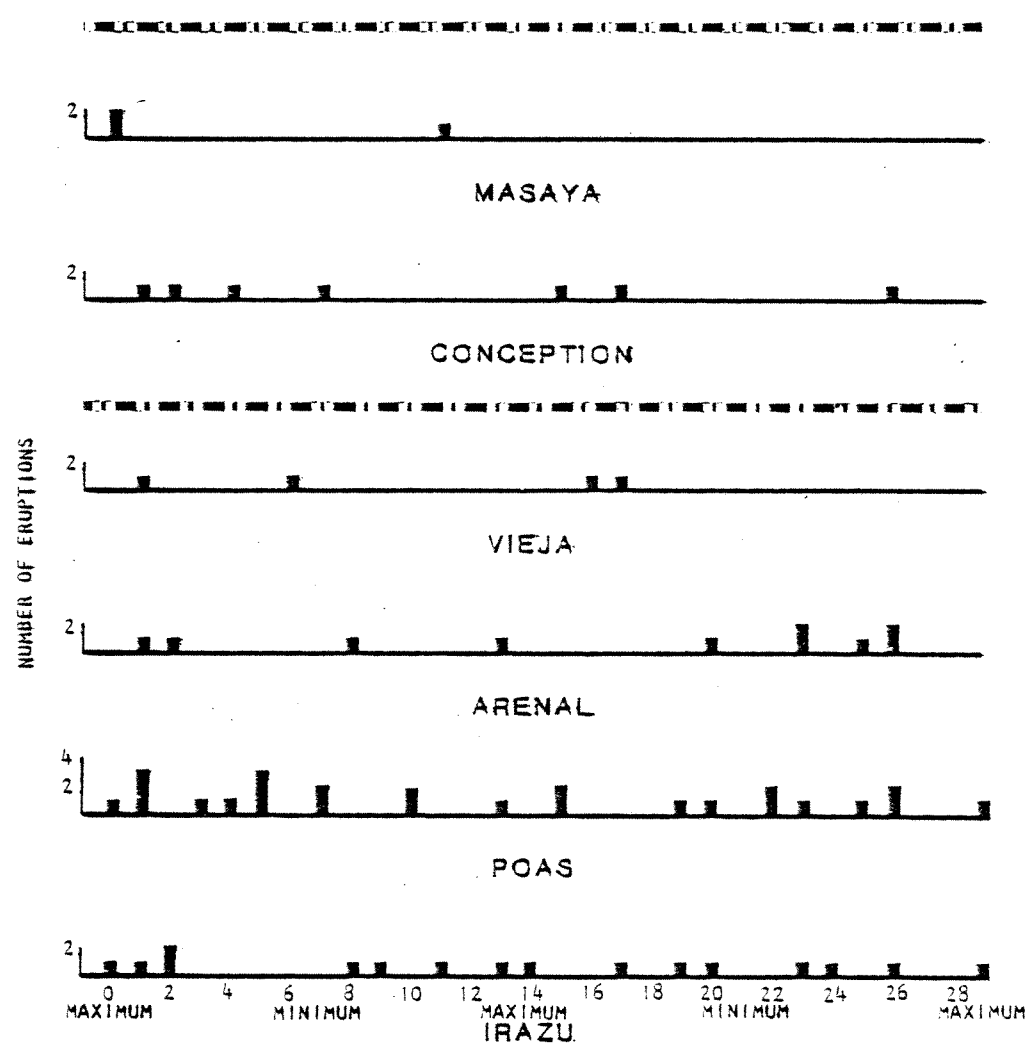
RESULTS

Full Cycles

The full cycle histograms for individual volcanoes (Figs. 3,4,5) indicate that there are no statistically significant correlations between 15 and 30 day tidal cycles and initial volcanic eruption times in Central America. There are no appreciable clusters at any part of the cycles in the total vector, north-south, synodic and anomalistic plots.

In Figure 6b, a single day peak occurred at perigee for the volcano San Cristobal. This seems rather insignificant since only five eruptions were important enough to consider for the time span from 1900 to the present. Notes from the Center for Short-Lived Phenomena classify two of the five eruptions as moderately weak.

In Figure 3c, a peak occurred 2 days after new moon at Santa Maria. The six eruptions for one day are two units greater than any other day and barely fall beyond 2σ from the mean (.4 eruptions). Although this



TOTAL VECTOR

DAY ZERO IS MEASURED FROM NEAREST SYNODIC DAY ZERO
Dashed lines represent segment breaks

FIGURE 3a

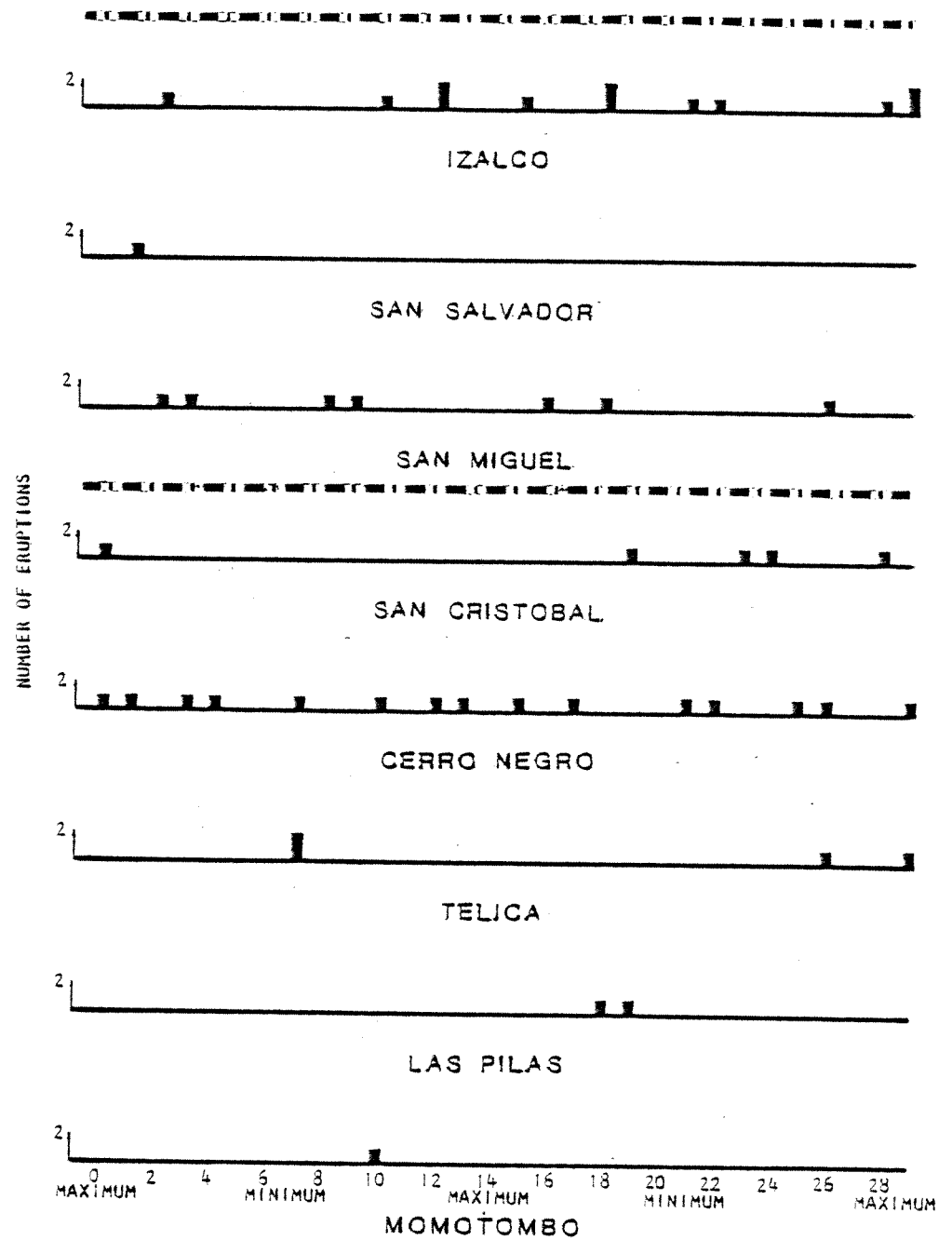


FIGURE 3b

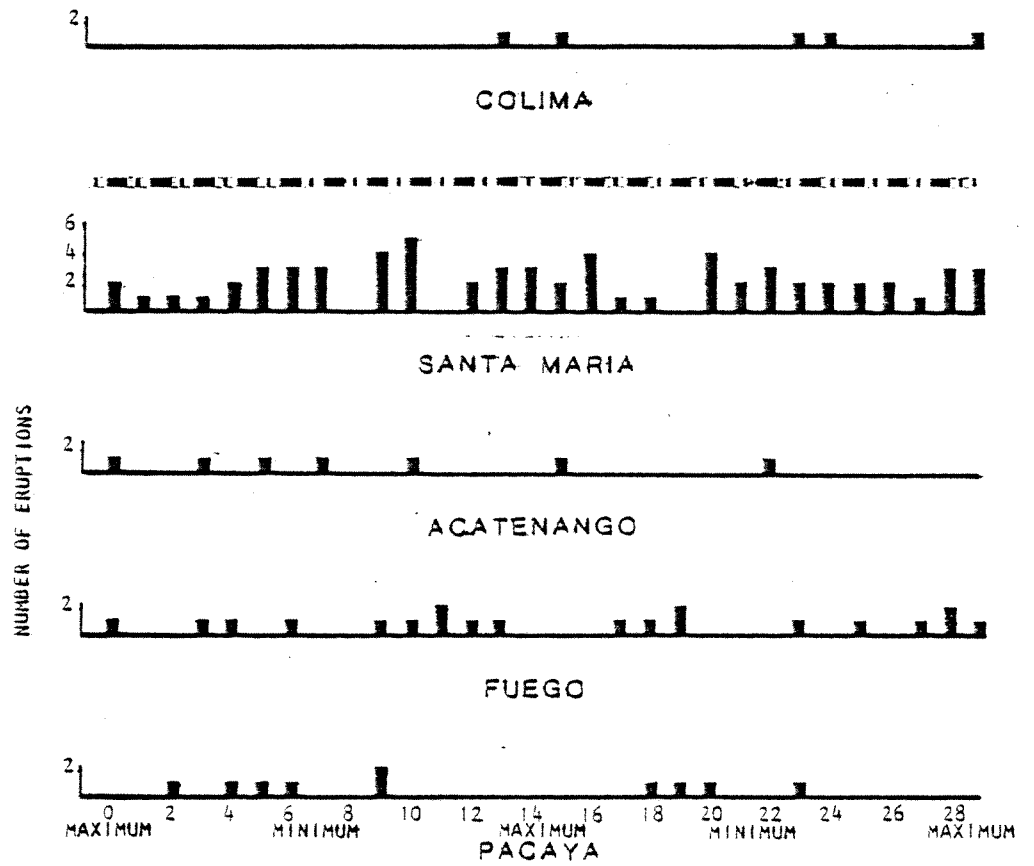
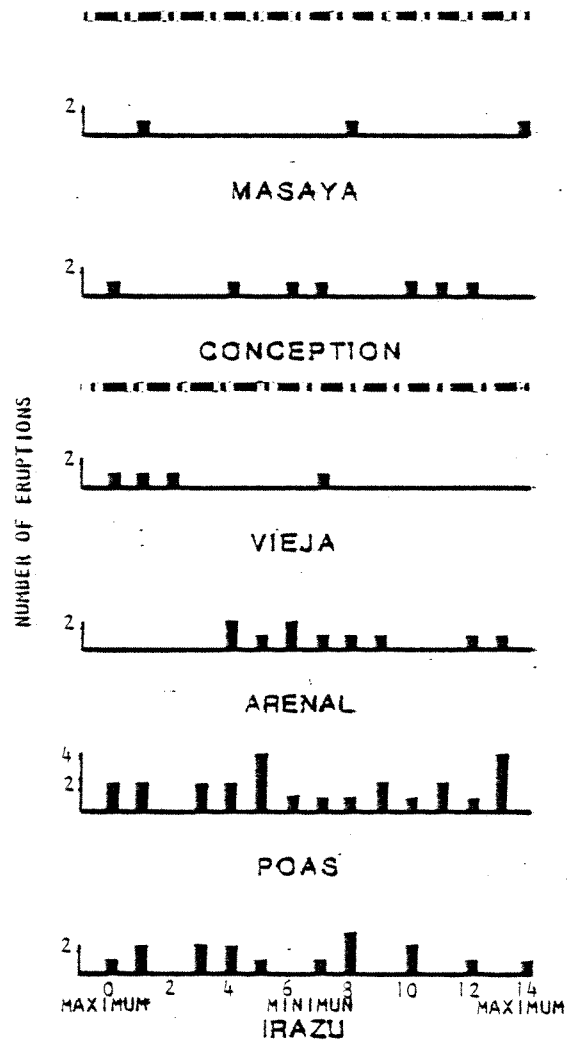


FIGURE 3c



NORTH-SOUTH
COMPONENT OF TIDAL ACCELERATION

FIGURE 4a

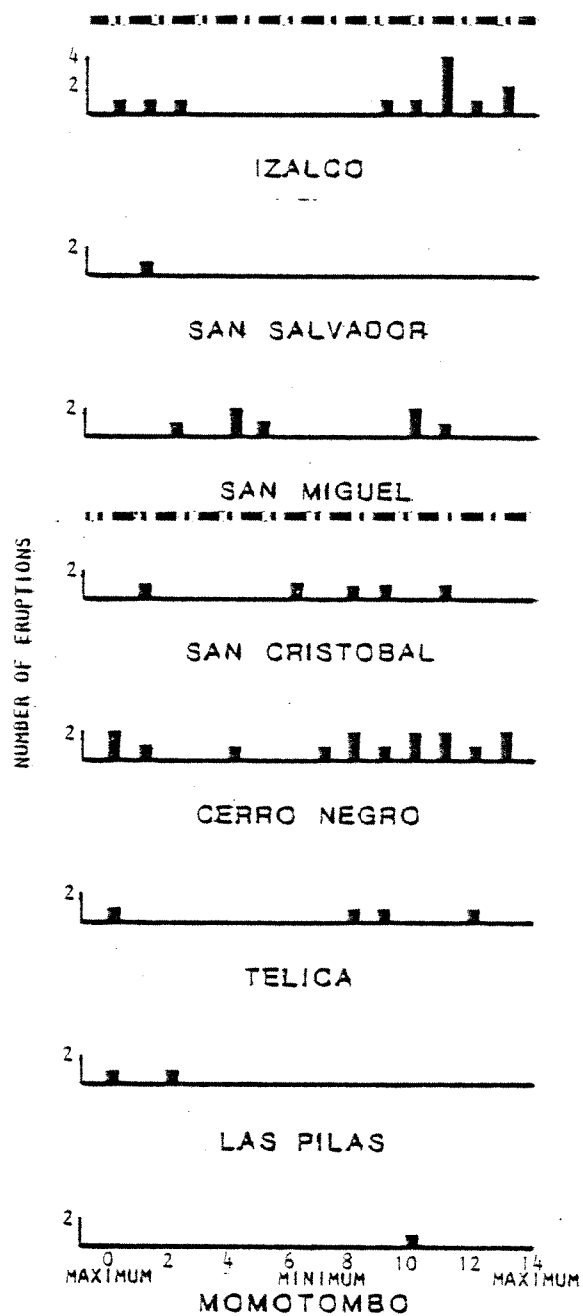


FIGURE 4b

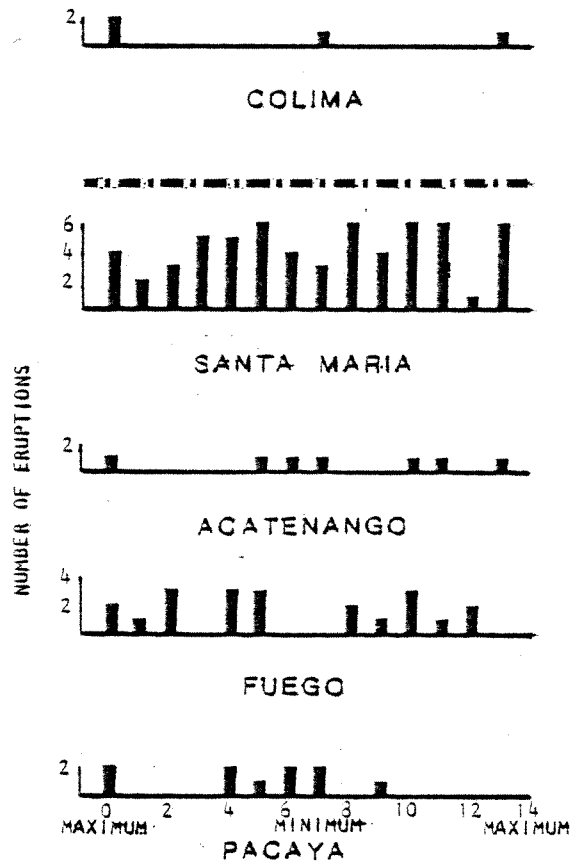
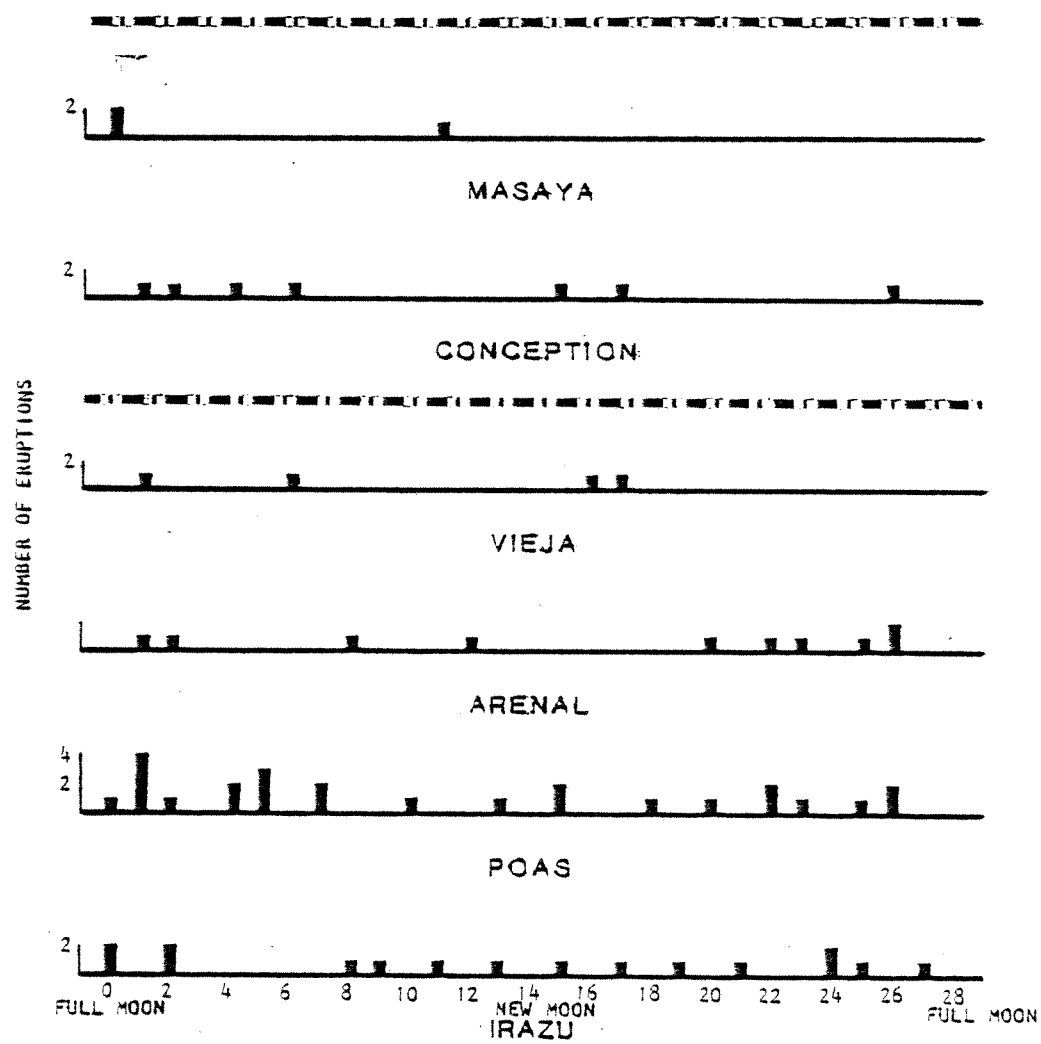


FIGURE 4c



SYNODIC

FIGURE 5a

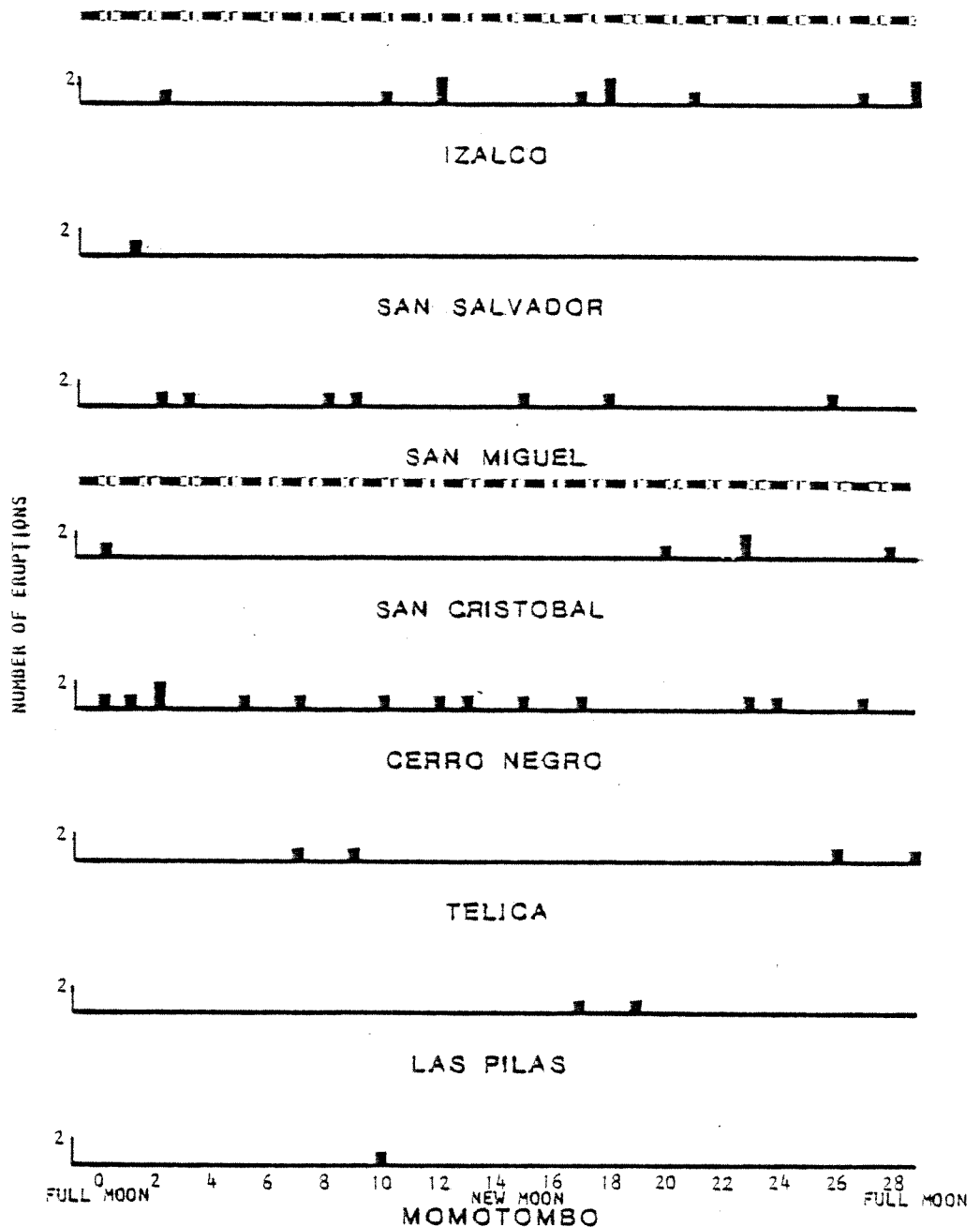


FIGURE 5b

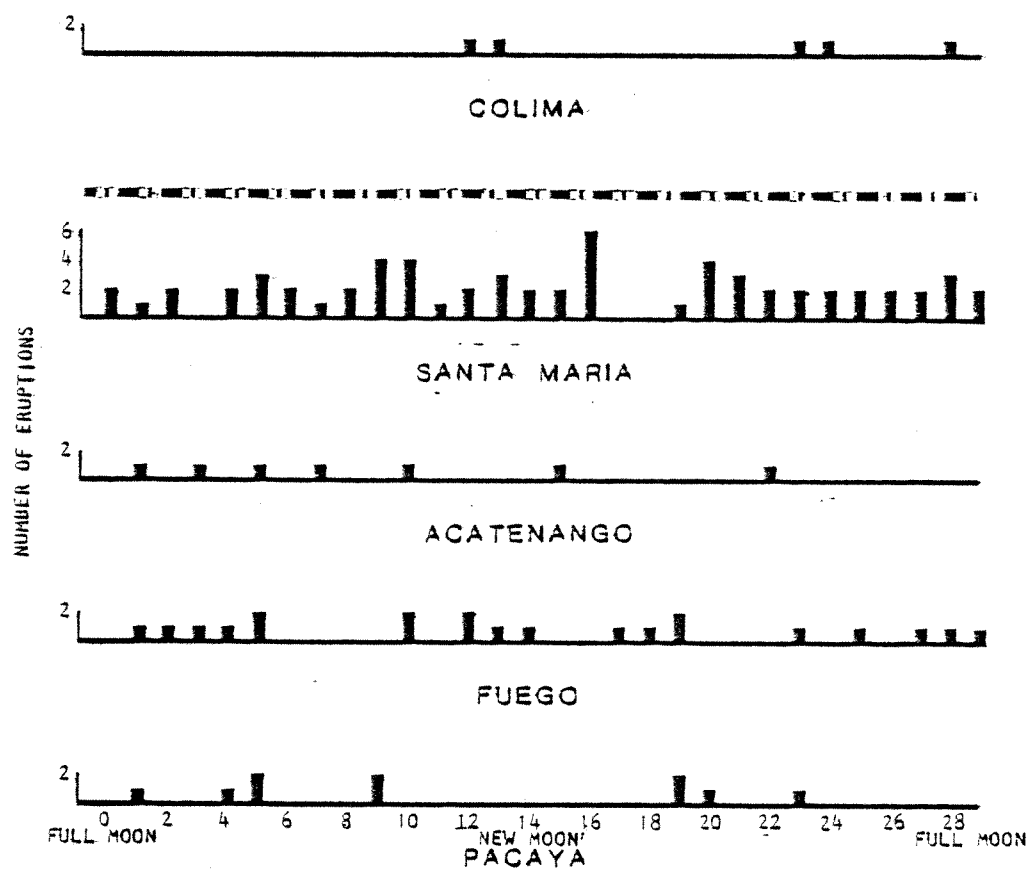
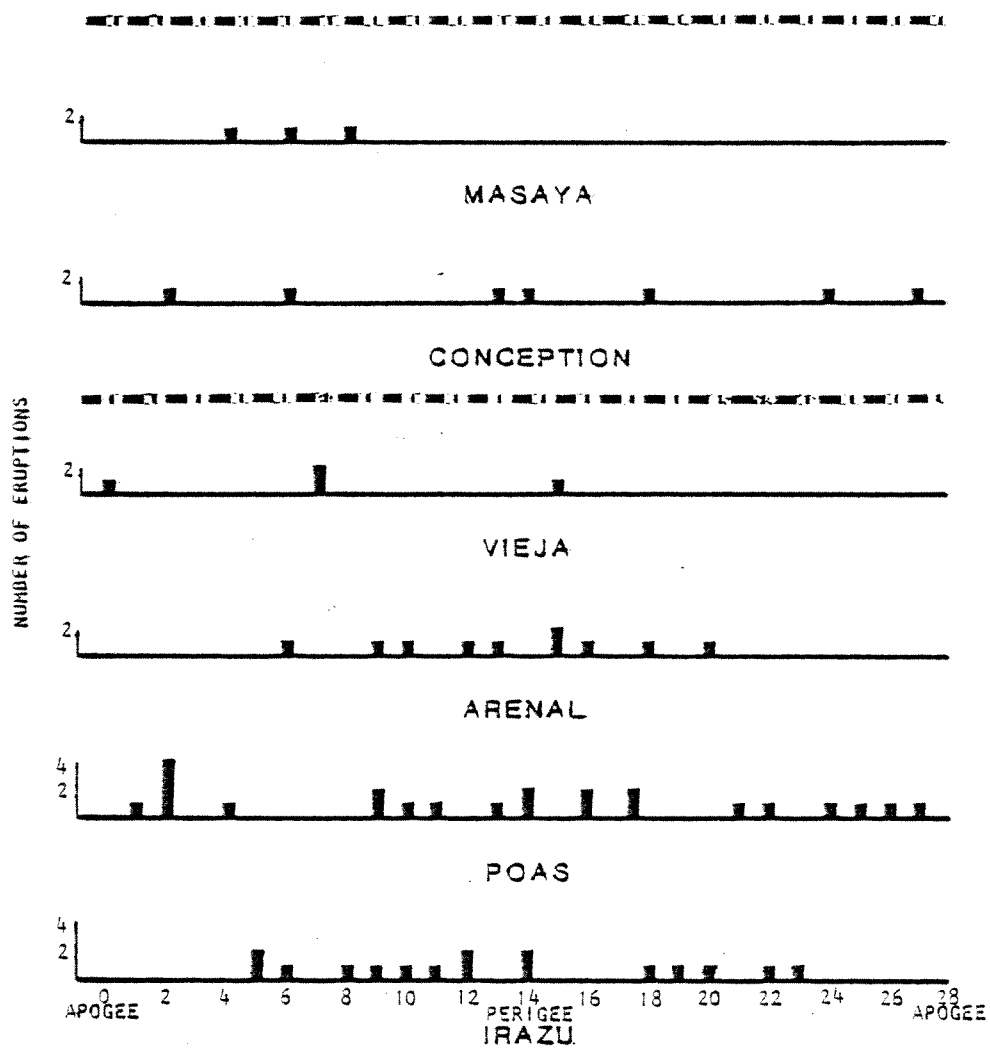


FIGURE 5c



ANOMALISTIC

FIGURE 6a

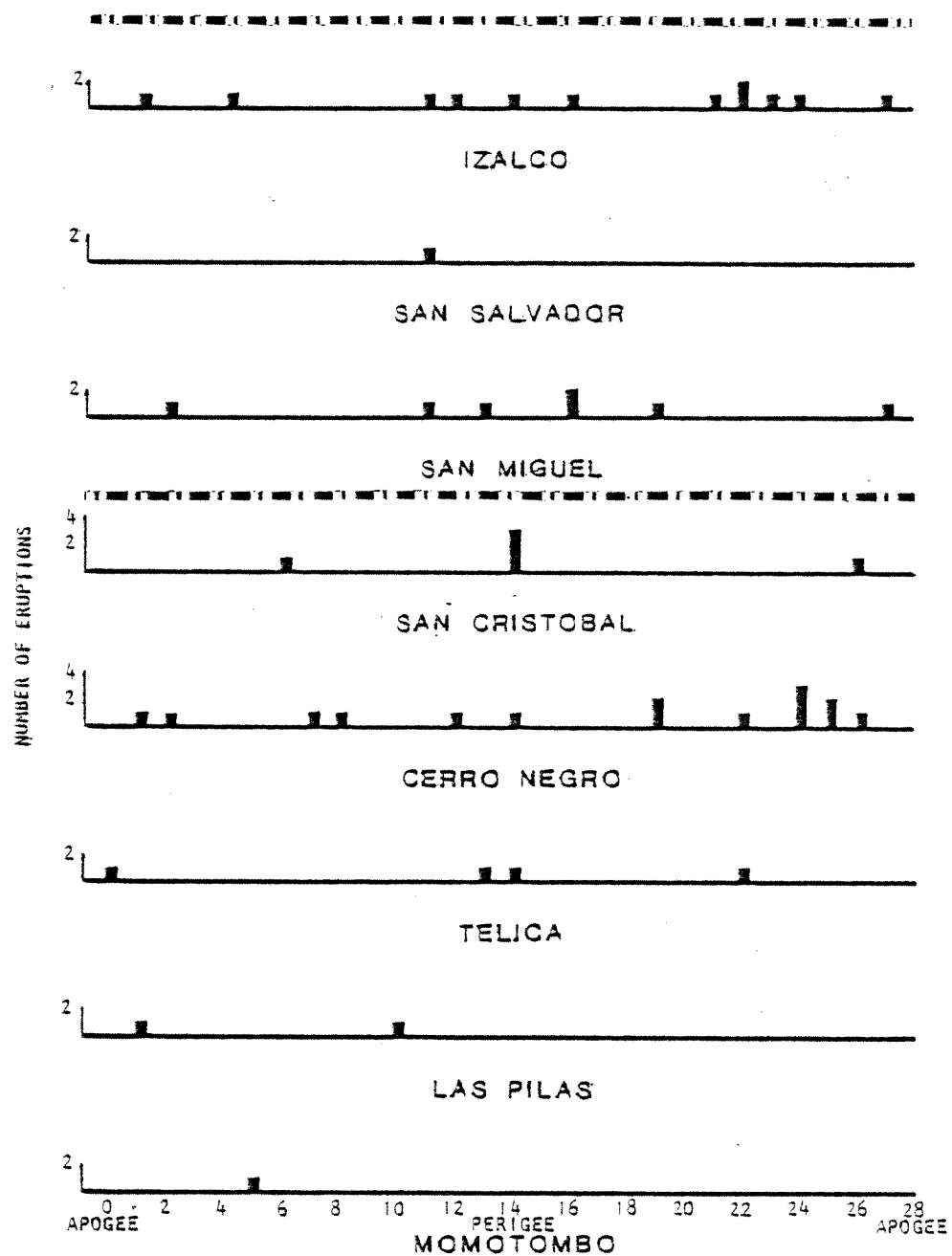


FIGURE 6b

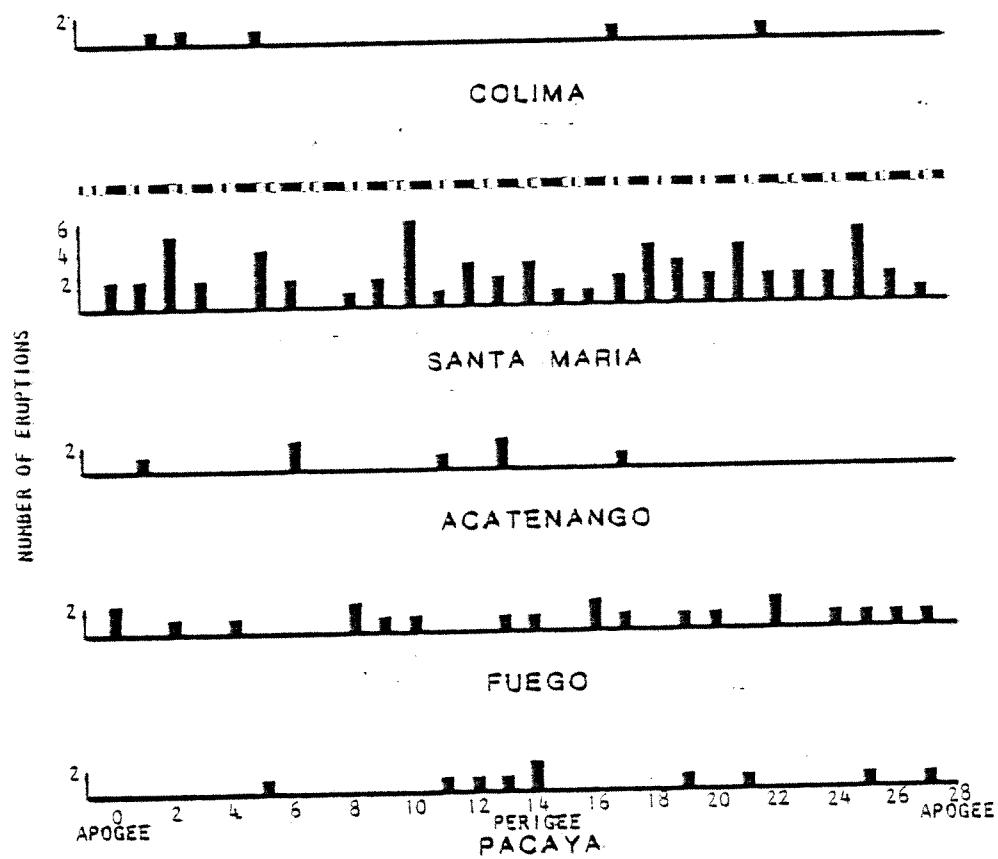


FIGURE 6c

indicates a valid correlation, a peak at a single day may be misleading, since the accuracy of eruption times are limited. A truer assessment can be made by averaging the eruption frequency of a given day with its two nearest neighbors. The apparent peak at day 16 for Santa Maria, when averaged with its neighbors, falls well within 1σ from the mean and therefore there is no significant correlation.

Reduced Cycles

The 8 day shortened north-south cycle for Poas appears in Figure 7. Peaks of eruption frequency occur at maximum and 2 days past minimum of the north-south cycle but are within 2σ of the mean. A peak at day 12 of the anomalistic cycle is beyond 2σ however, when averaged with its neighbors, it falls well below that level.

Eruptions for all volcanoes were added for all cycles in Figures 8 through 11. Again, no clusters were significant.

The problem of additive days missing for reduced cycles was addressed in the methods sections and will be clarified here. Two eruption units beyond 2σ occur at perigee for all eruptions of the anomalistic cycle of Figure 11. Values at perigee may be higher than shown on the reduced cycles, however, the full cycle (histogram A) peak at perigee is probably lower. Four or five sets of two successive days each shared the exact same acceleration in microgals. This occurred at perigee and made it difficult to determine whether an eruption occurring near perigee was exactly one or two days from lowest acceleration. Therefore a wider range for perigee resulted and some eruptions assigned to perigee may fall on the day before or after. The clustering test shows that the observed peak is within the boundaries of randomness. The asterisks on the reduced cycles at perigee and minimum acceleration on the north-south cycles indicate that eruption units are probably higher than

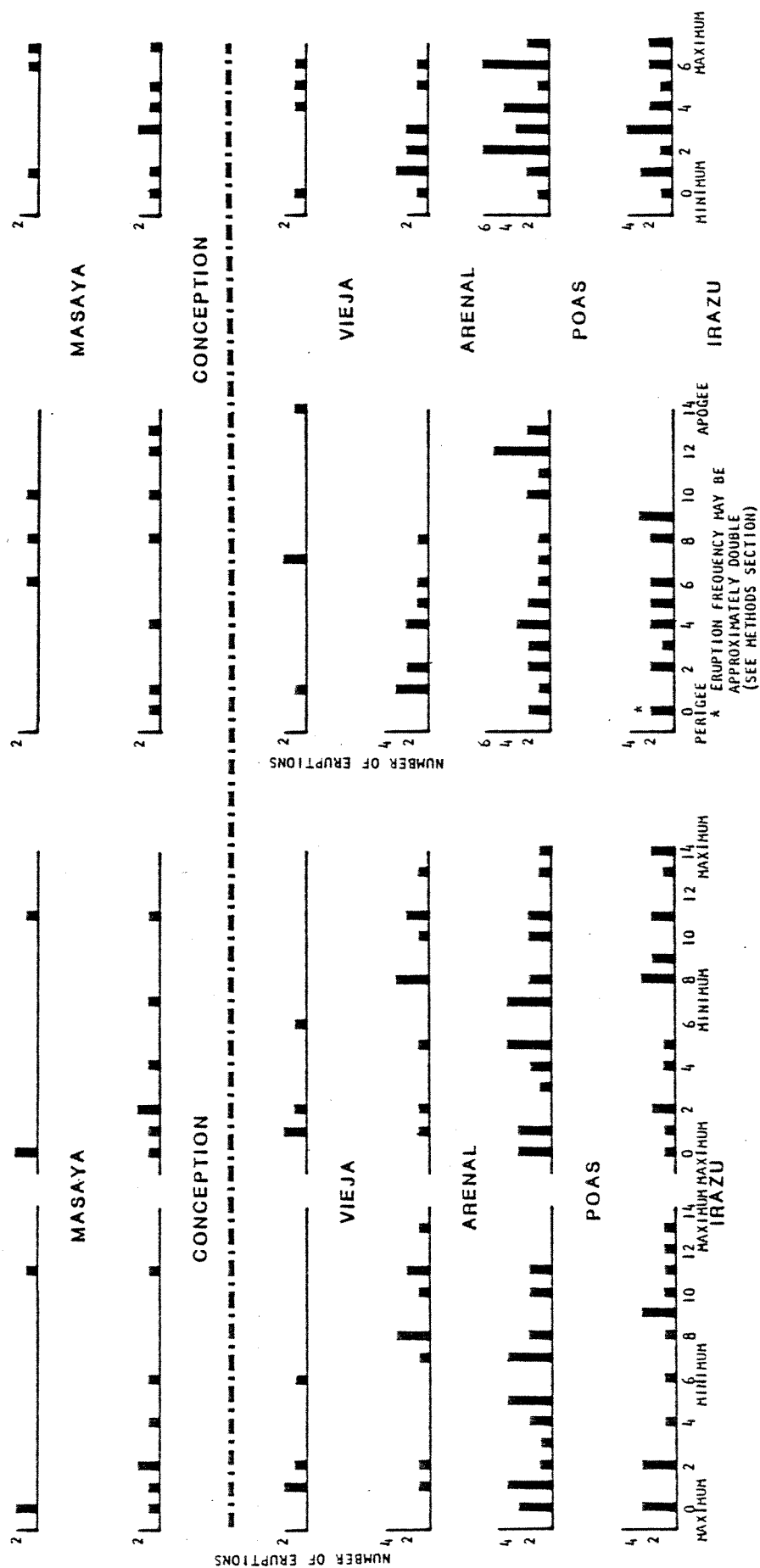


Figure 7a

REDUCED CYCLES

15 DAY CYCLE 15 DAY CYCLE 8 DAY CYCLE

Synodic Total Vector Anomalistic North-South

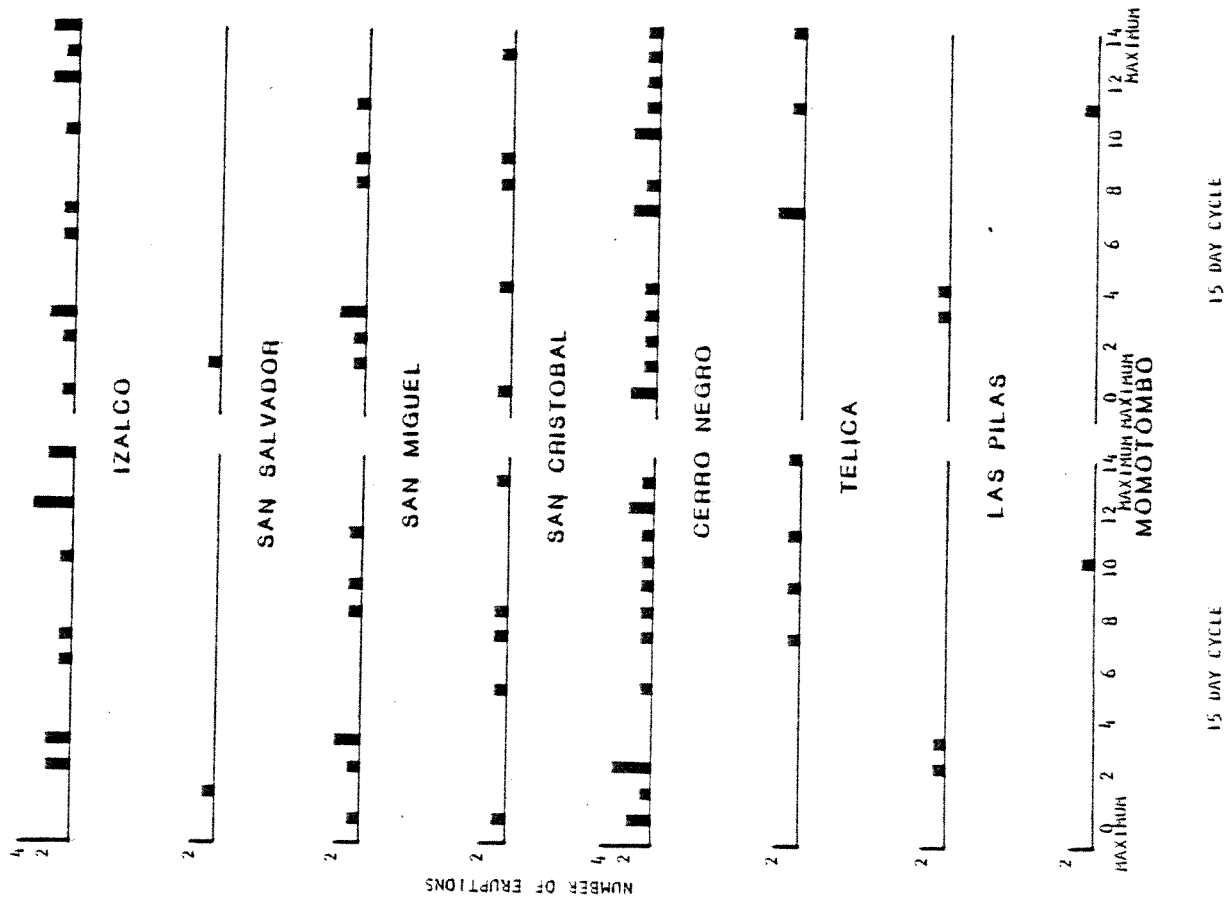
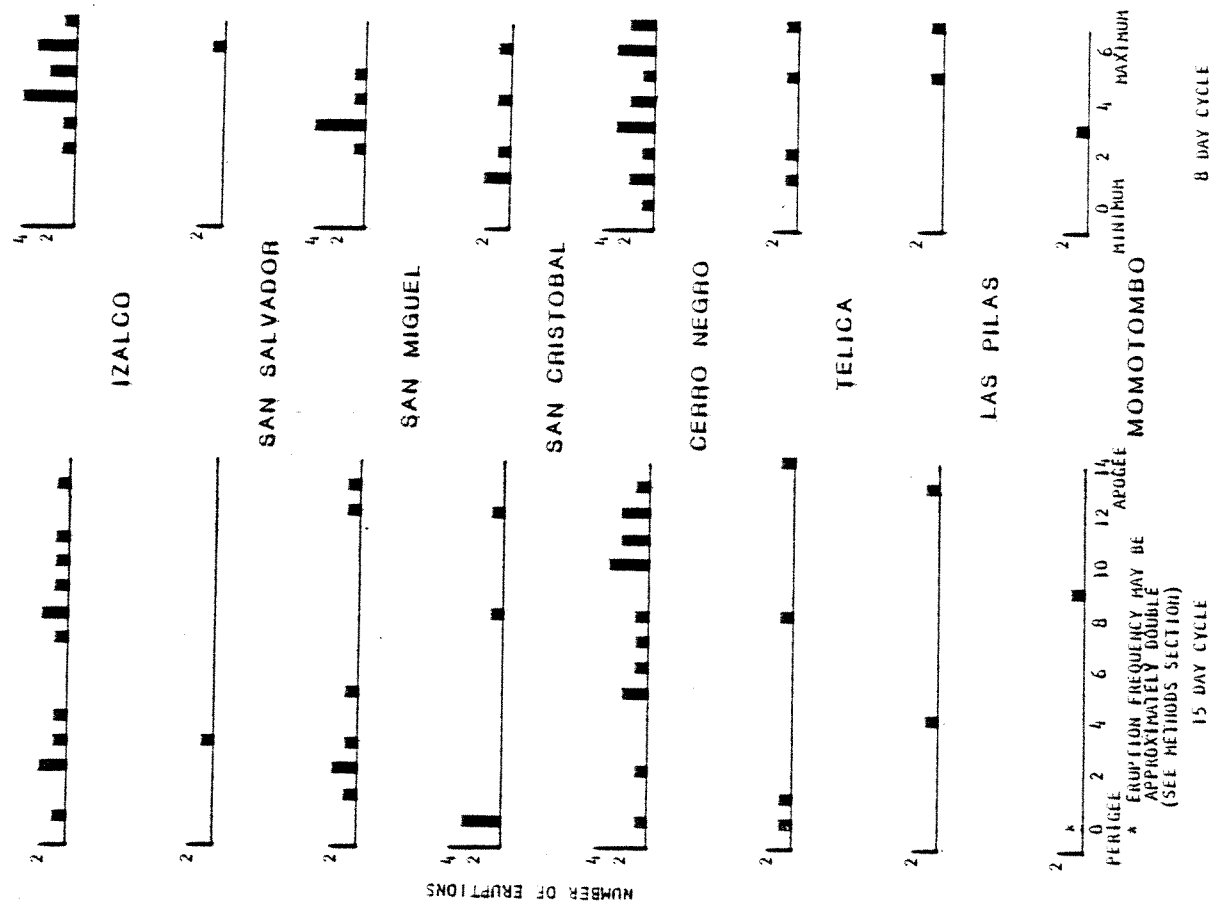


Figure 7b



MOMOTOMBO

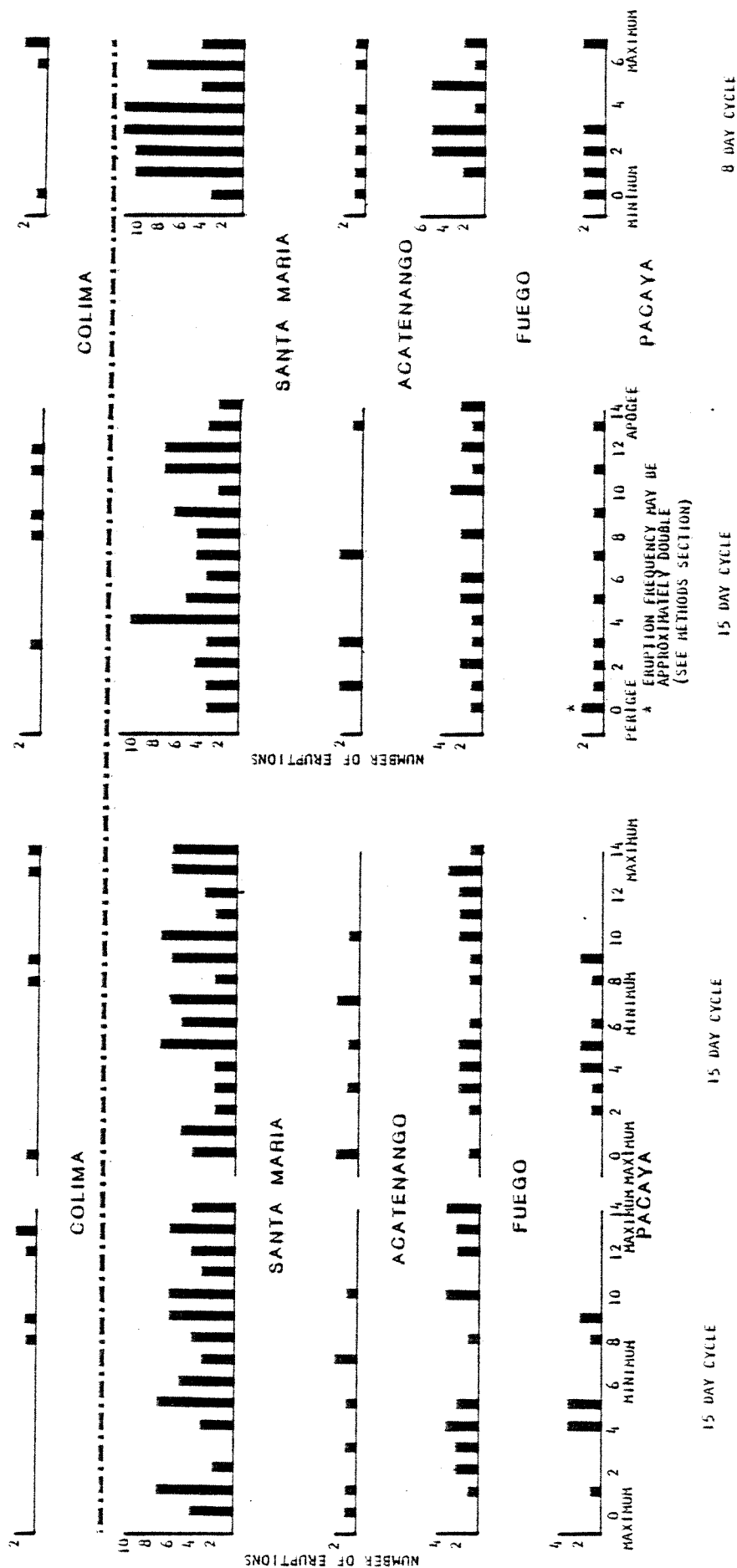
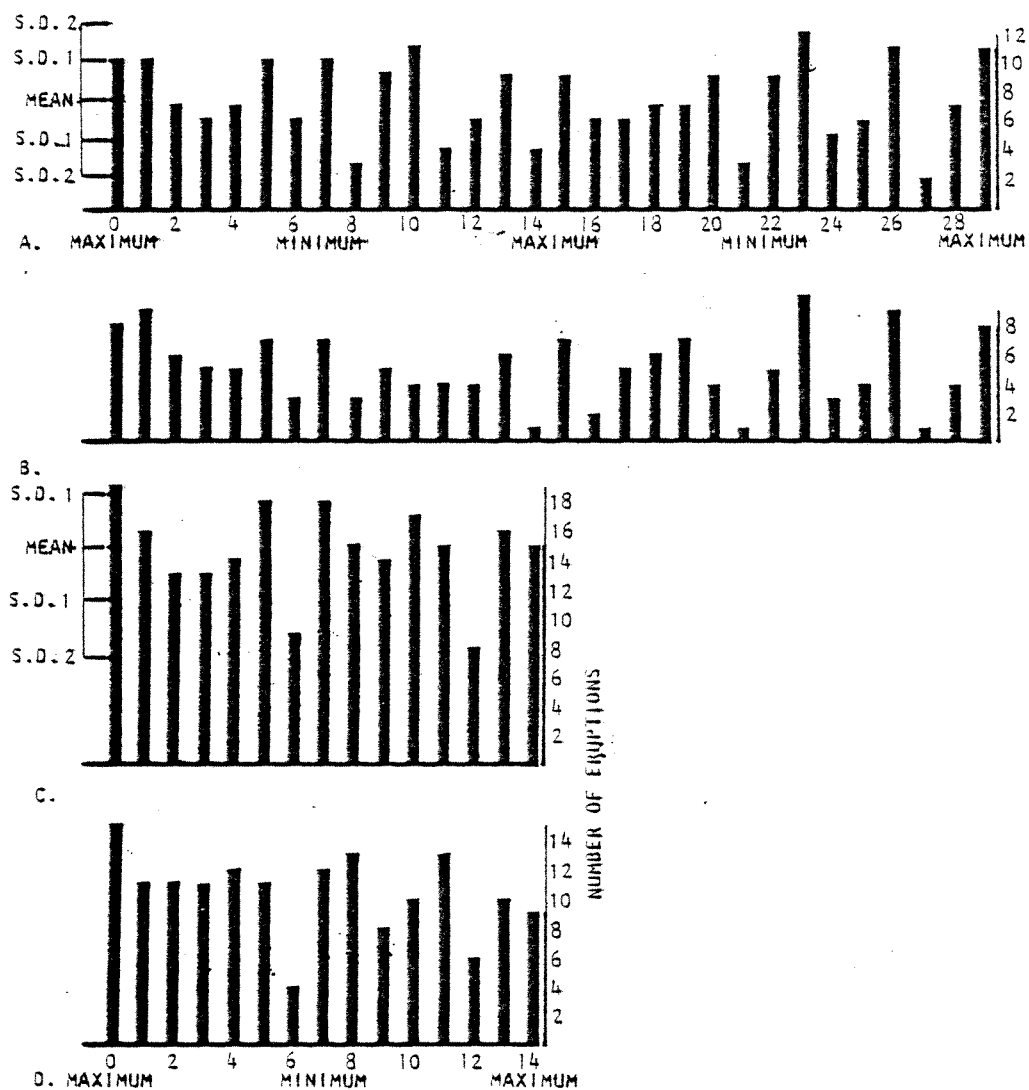


Figure 7c

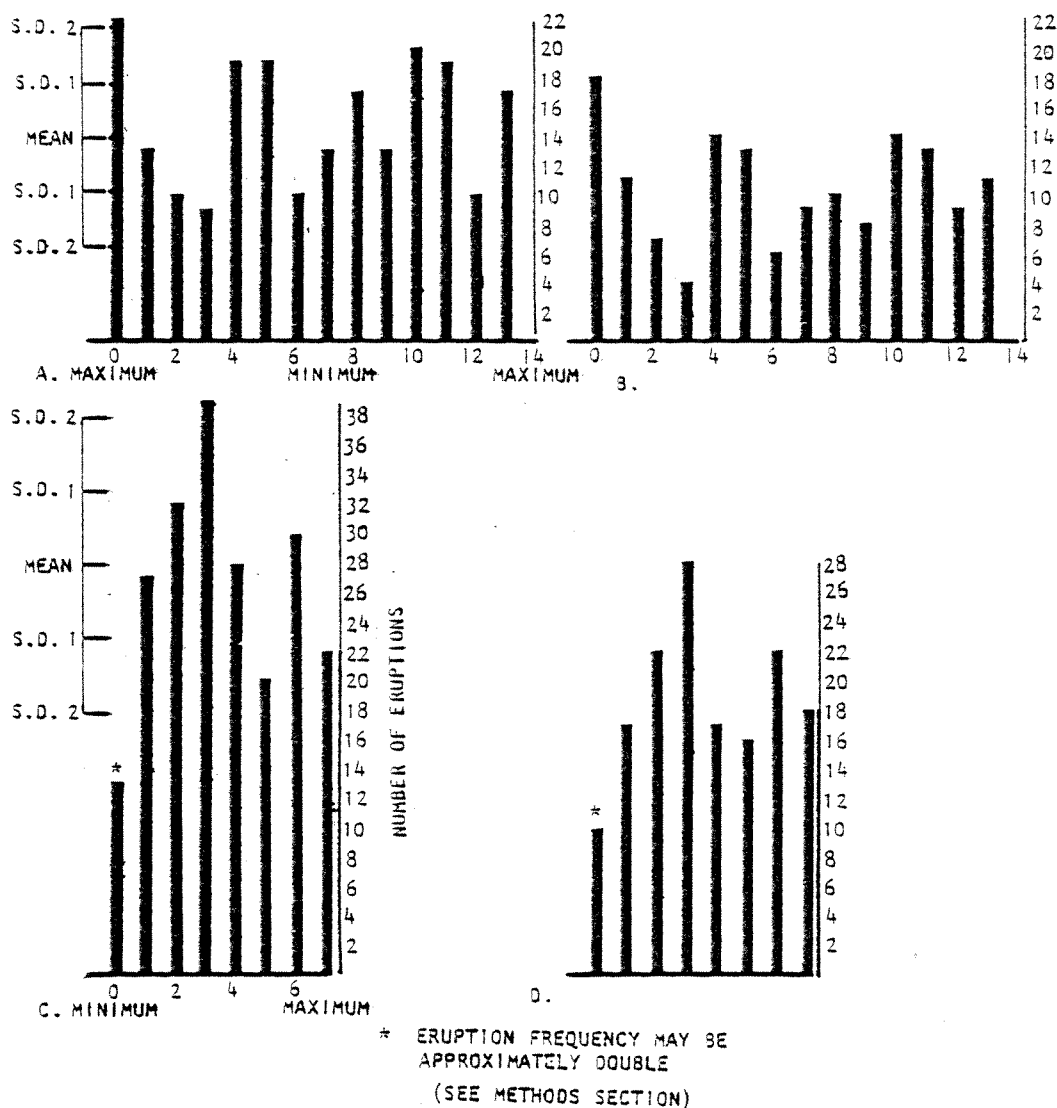


TOTAL ERUPTIONS-TOTAL VECTOR

SHOWING MEAN AND STANDARD DEVIATION

- A. ALL ERUPTIONS
- B. ERUPTIONS MINUS SANTA MARIA
- C. 15 DAY CYCLE
- D. 15 DAY CYCLE MINUS SANTA MARIA

FIGURE 8

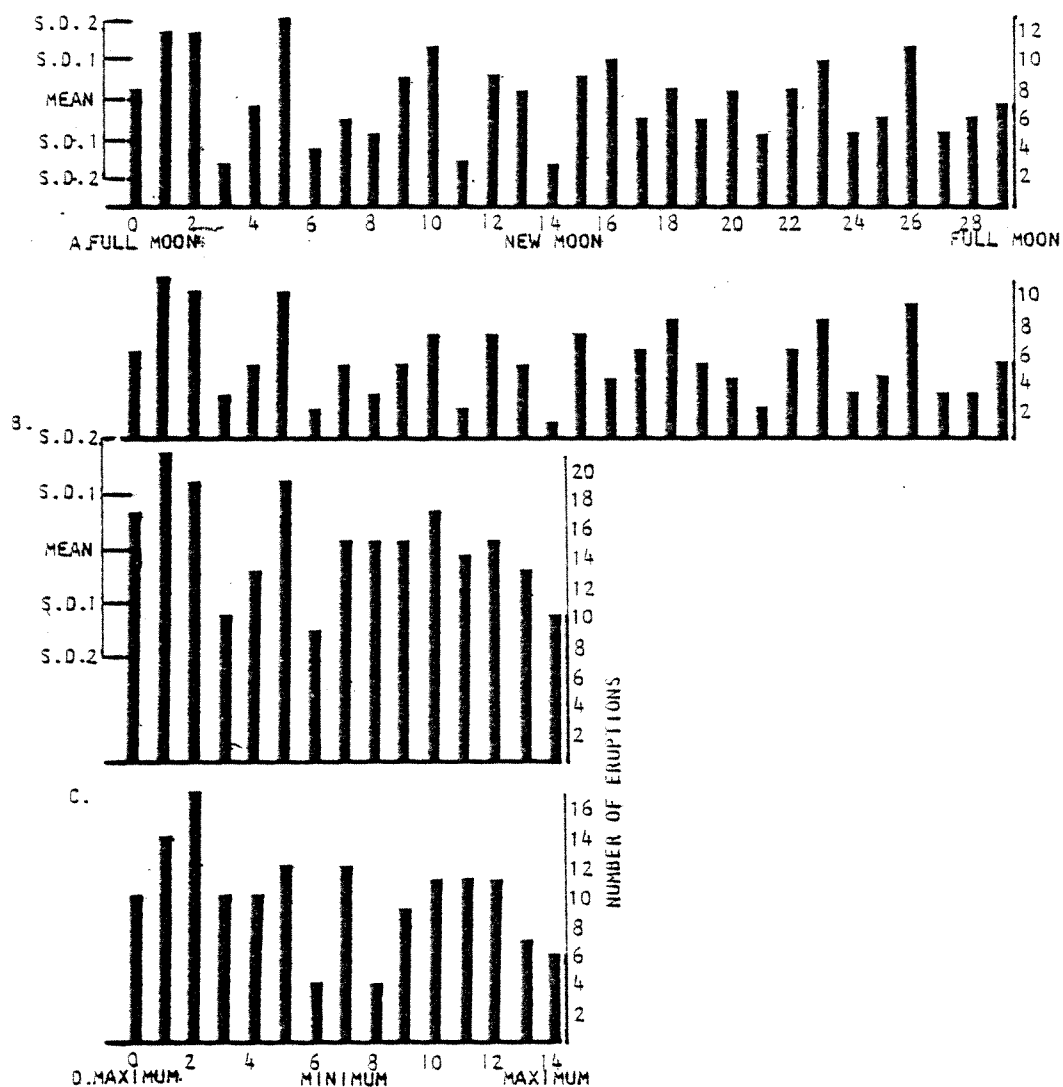


TOTAL ERUPTIONS - NORTH-SOUTH

SHOWING MEAN AND STANDARD DEVIATION

- A. ALL ERUPTIONS
- B. ERUPTIONS MINUS SANTA MARIA
- C. 8 DAY CYCLE
- D. 8 DAY CYCLE MINUS SANTA MARIA

FIGURE 9

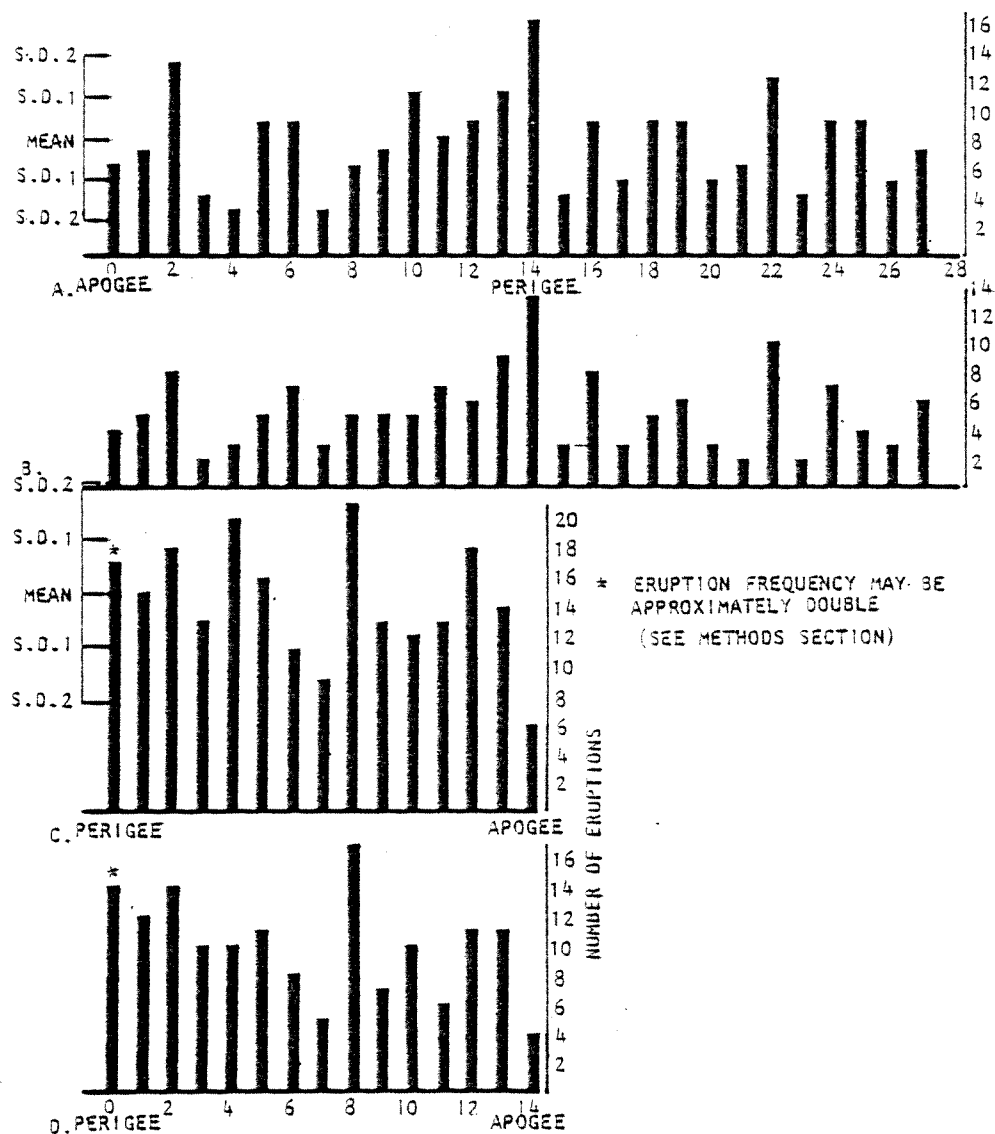


TOTAL ERUPTIONS-SYNODIC

SHOWING MEAN AND STANDARD DEVIATION

- A. ALL ERUPTIONS
- B. ERUPTIONS MINUS SANTA MARIA
- C. 15 DAY CYCLE
- D. 15 DAY CYCLE MINUS SANTA MARIA

FIGURE 10



TOTAL ERUPTIONS - ANOMALISTIC

SHOWING MEAN AND STANDARD DEVIATION

- A. ALL ERUPTIONS
- B. ERUPTIONS MINUS SANTA MARIA
- C. 15 DAY CYCLE
- D. 15 DAY CYCLE MINUS SANTA MARIA

FIGURE 11

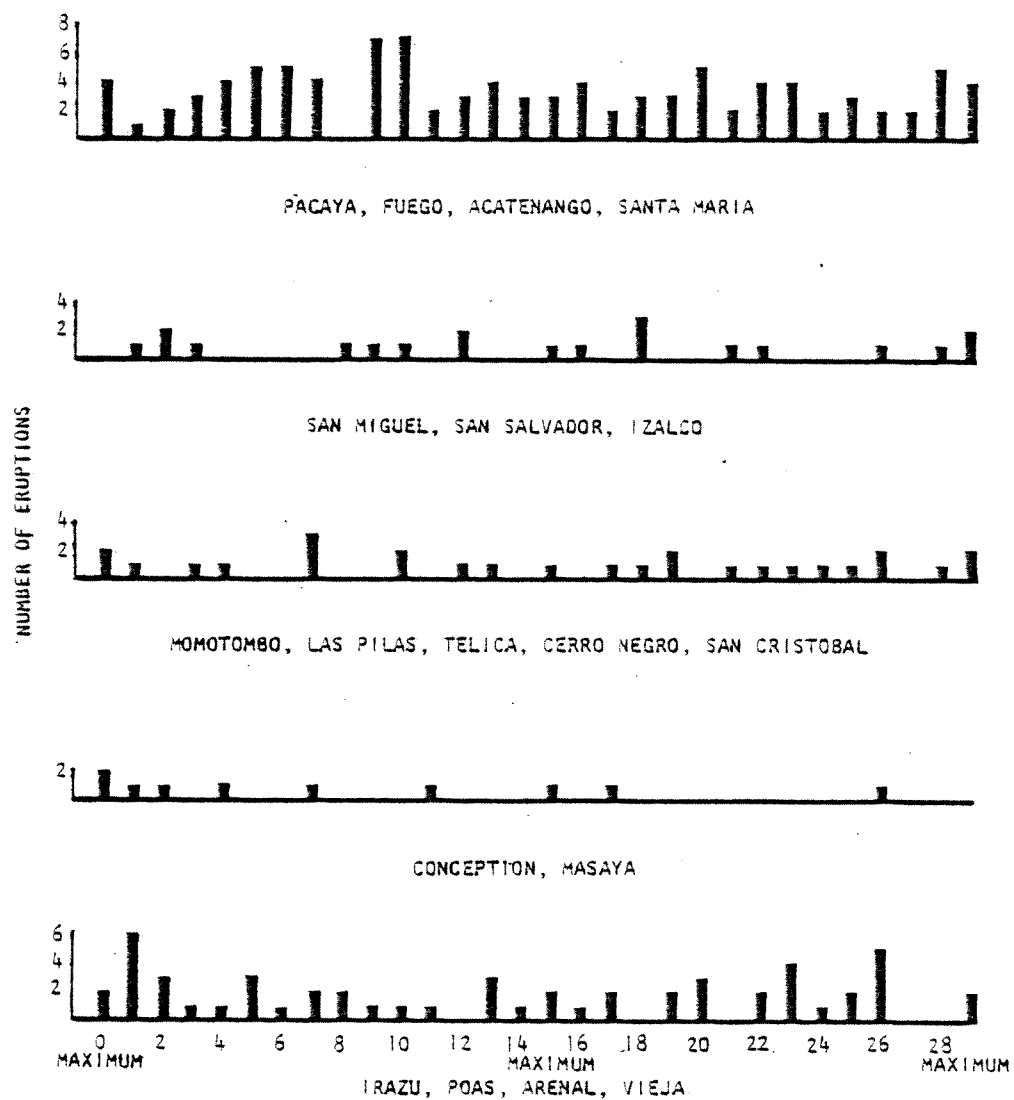
shown and maximally may be double. Since perigee peaks are most likely lower than depicted on the histograms, doubling them would be misleading. Adding perhaps 20% would be more realistic (Fig. 11). In Figure 9, the eruption days for day zero (minimum acceleration) would probably be close to double its observed value because unlike the eruption units of perigee, its values are depicted accurately.

Effects of Segments

The total vector histograms of Figure 12 are sums of eruptions representing volcanoes of five different segments. Segments are areas of approximately the same location and structure which would be expected to experience similar tidal effects. If earth tides trigger volcanic eruptions, similarity in eruptive characteristics among volcanoes of the same segment should be evident. Hence, volcanoes of the same segment should erupt at the phase of the tidal cycle. A major consideration is that volcanoes of the same segment need not be at the same critical state; therefore, they should not necessarily erupt on the same day. However, they should erupt on similar days separated by months and perhaps years. The actual eruptions may lag many days after an amplitude peak, or occur at any time during the lunar cycle, but the important criterion is that the frequency of eruptions should cluster in time.

Only one day of the total vector cycle for one segment was notable. The segment including the volcanoes Irazu, Poas, Arenal, and Vieja showed a peak at day one (beyond maximum amplitude acceleration) of 6 eruptions. This corresponds to 1.56 units greater than 2σ from the mean. When averaged with the day before and after, the cluster is only .5 units from the mean and within 1.4 units of 1σ .

This randomness in the frequency of eruption throughout the indi-



TOTAL VECTOR
SUM OF ERUPTIONS PER SEGMENT

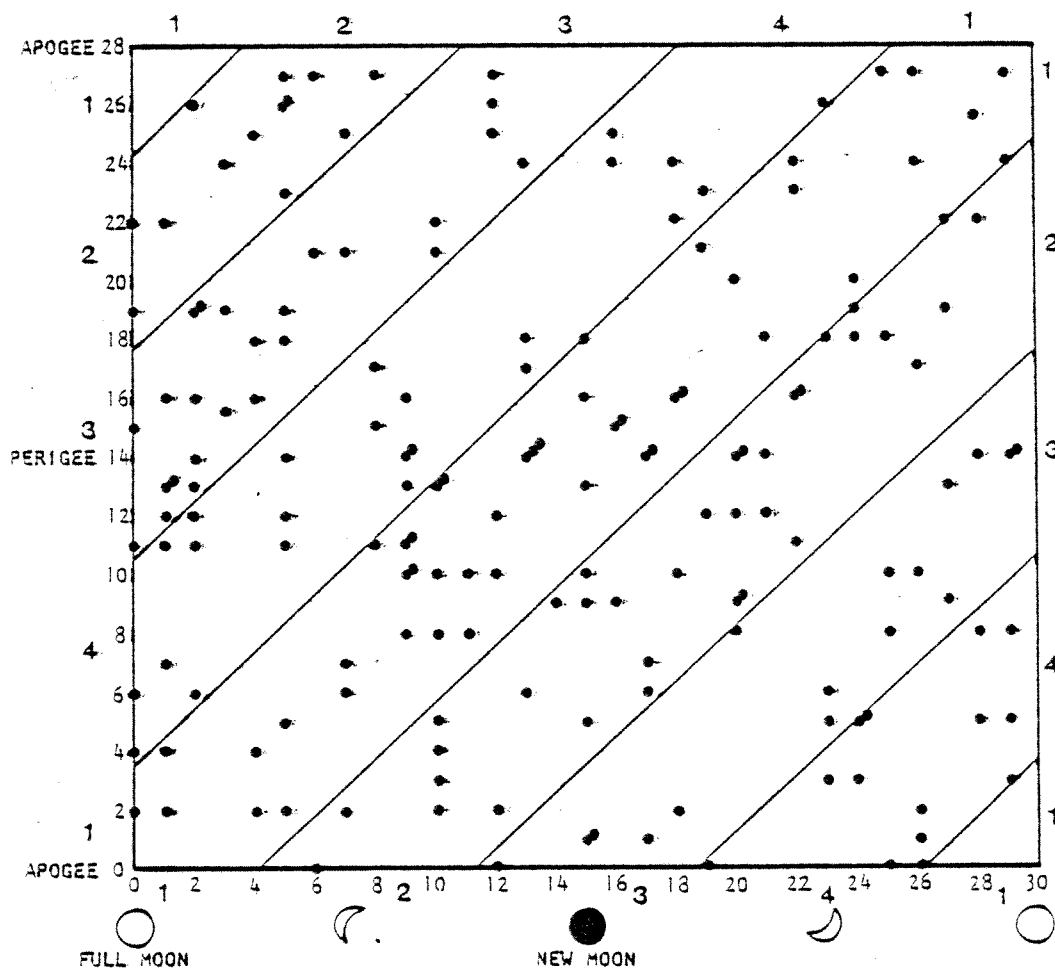
FIGURE 12

vidual segments fails to reinforce the theory of Stoiber and Carr, but, due to the lack of tidal eruption correlation evidenced by Figures 3 through 5, this randomness offers no valid inferences to the segmented nature of Central America.

Synoptic and Monthly Analysis

Figure 13 shows randomness in the evaluation of tidal triggering by the association of the synodic and anomalistic months. 51% of the eruptions occurred when the synodic and anomalistic cycles were within about one week of phase synchronization, and 49% occurred at 90° and 270° phase lags. Hamilton's positive correlations may be due, in part, to his source of volcanic eruptions data, namely Lamb's (1970) and the Smithsonian Center for Short Lived-Phenomena's lists of world-wide eruptions from 1880 to 1971. These lists are incomplete and stress only the largest eruptions. The eruption times used in this study were cross checked for accuracy from many sources and were limited to years from 1900 to the present for eruptions in Central America

Figure 14 groups the total eruptions into calendar months and subgroups them by occurrence in the dry or rainy season. Initially it was observed that the frequency of eruptions increased from September to February and that the phenomenon might be coincidental with the dry season. Average monthly rainfall vary little from year to year; the rainy season begins near the beginning of May and ends by late October (Stoiber et al., 1975). Although the eruptions of the dry season outnumber those of the rainy season, the difference is inconsequential. There is a strong tendency for eruptions to occur from September to February. 57% of all eruptions occur during those months whereas 42.2% occur during the dry season. Although the reason for the slight



SYNODIC VS. ANOMALISTIC

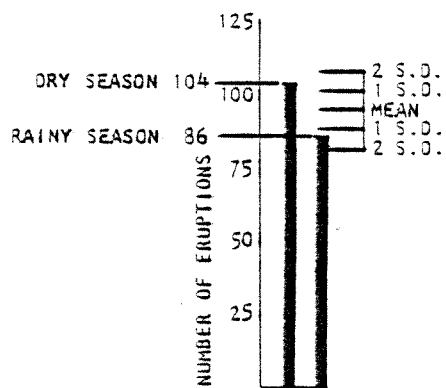
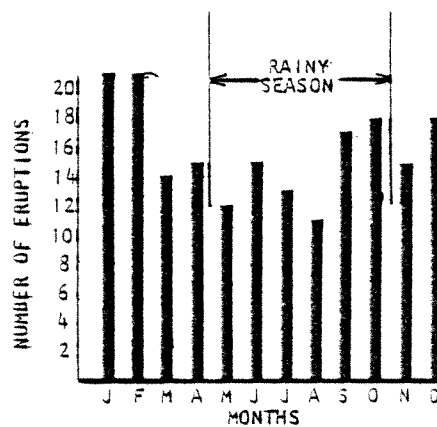
BANDS DESCRIBE A WEEK CENTERED AROUND EACH QUARTER PHASE

BAND 1. FULL MOON AND APOGEE IN PHASE

BAND 3. NEW MOON AND APOGEE IN PHASE

BANDS 2 AND 4. CYCLES OUT OF PHASE

FIGURE 13



TOTAL ERUPTIONS-CALENDER MONTHS

SHOWING MEAN AND STANDARD DEVIATION

FIGURE 14

increase is uncertain, statistical tests indicate it is within the bounds of randomness.

CONCLUSION

There is no statistically significant correlation between the phases of the solid earth tides and the beginnings of volcanic eruptions in Central America.

APPENDIX I

Irazu

09.59, -83.51

Eruption date	Total Vector	North-South	Synodic	Anomalistic
27 Dec 1917	0	+7	0	22
30 Jan 1918	24	+3	25	18
25 July 1918	1	-2	2	12
9 Aug 1962	23	+1	24	5
2 Apr 1963	23	-6	24	20
17 Apr 1963	9	-4	9	8
9 June 1963	2	-6	2	6
25 June 1963	19	-3	19	23
3 Sept 1963	29	-3	0	11
14 Jan 1964	14	-7	15	5
18 Feb 1964	20	+1	21	12
23 Mar 1964	26	-4	27	19
14 Apr 1964	17	+3	17	14
6 June 1964	11	+1	11	10
2 July 1974	8	0	8	9
7 July 1964	13	+5	13	14

Poas

10.12, -84.13

25 Jan 1910	0	-6	1	22
30 May 1914	20	-2	20	9
8 Oct 1914	3	+6	4	2
25 Dec 1951	5	-2	5	26
23 May 1963	1	+5	1	16

Eruption date	Total Vector	North-South	Synodic	Anomalistic
2 July 1963	26	+3	26	1
25 Dec 1964	7	0	7	21
1 Jan 1967	5	-2	5	14
3 May 1969	1	-7	1	13
3 June 1969	4	-2	4	16
9 Feb 1972	10	+6	10	4
14 Feb 1972	15	-3	15	9
27 May 1972	29	+6	0	2
9 June 1972	13	+4	13	14
18 June 1972	22	+1	22	24
21 June 1972	25	+4	25	27
27 Oct 1972	5	-4	5	18
9 Nov 1972	19	-6	18	2
25 Jan 1973	7	+2	7	25
28 Jan 1973	10	+5	10	28
9 Feb 1973	22	+6	22	11
3 Apr 1973	15	+2	15	10
11 Apr 1973	23	-3	23	18
8 Sept 1973	26	-4	26	2

Arenal

10.27, -84.42

29 July 1968	20	-1	20	9
1 Aug 1968	23	+2	23	12
4 Aug 1968	26	+6	26	15
10 Aug 1968	2	-2	23	12
14 Sept 1968	8	+6	8	15

Eruption date	Total Vector	North-South	Synodic	Anomalistic
19 Sept 1968	13	-3	12	6
1 Oct 1968	25	-3	25	18
3 May 1969	1	+5	1	13
13 Apr 1973	26	0	26	10
17 June 1975	23	+1	22	16

Vieja

10.50, -85.21

15 Sept 1966	6	0	6	0
29 Nov 1966	1	-7	1	7
10 June 1967	17	-5	17	7
22 Apr 1969	6	-6	6	0

Conception

11.32, -85.39

2 Apr 1957	17	+4	17	6
28 Nov 1961	7	-3	6	27
9 May 1963	1	+5	1	2
24 Dec 1973	15	-7	15	13
12 Jan 1974	4	-1	4	18
5 Apr 1977	2	+3	2	14
29 Apr 1977	26	0	26	24

Masaya

11.57, -86.09

27 Feb 1927	11	-6	11	8
13 July 1946	0	+7	0	4

Eruption date	Total Vector	North-South	Synodic	Anomalistic
10 Oct 1965	0	+1	0	6
Momotombo				
12.25, -86.33				
16 Jan 1905	10	+3	10	5
Las Pilas				
12.29, -86.41				
23 Oct 1952	19	-5	18	10
29 Oct 1954	18	-7	17	1
Telica				
12.36, -86.42				
16 Jan 1965	29	+7	29	14
24 Jan 1965	7	+1	7	22
11 Feb 1969	7	+5	9	13
3 Nov 1976	26	+2	26	0
Cerro Negro				
12.31, -86.44				
12 June 1947	10	+2	10	8
21 Nov 1950	12	+3	12	25
17 Dec 1950	22	+1	23	24
4 Sept 1957	25	-6	26	24
24 Sept 1957	15	+2	15	12
25 Oct 1961	3	+6	2	19
27 Mar 1962	7	+6	7	7
24 Oct 1968	17	+4	17	14

Eruption date	Total Vector	North-South	Synodic	Amomalistic
6 Dec 1968	1	+6	2	1
21 Dec 1969	13	+5	13	24
3 Feb 1971	23	0	24	19
6 Feb 1971	26	0	27	22
9 Feb 1971	29	+3	30	25
10 Feb 1971	0	+4	1	26
14 Feb 1971	4	+7	5	2

San Cristobal

12.42, -87.00

3 May 1971	23	-1	23	26
30 Nov 1971	28	+4	28	14
9 Mar 1976	24	-6	23	6
16 Mar 1976	30	+1	30	14
29 Aug 1976	19	+2	20	14

San Miguel

13.26, -86.16

10 Dec 1919	3	-3	3	19
14 Aug 1920	10	-3	15	16
23 Oct 1964	2	+4	2	13
22 Feb 1966	18	-2	18	2
5 Jan 1967	9	+3	9	16
30 Mar 1970	8	-5	8	11
2 Dec 1976	26	+3	26	27

San Salvador

13.44, -88.17

Eruption date	Total Vector	North-South	Synodic	Anomalistic
6 June 1917	1	-6	1	11

Izalco

13.49, -89.34

10 May 1902	18	-4	18	16
30 Dec 1902	15	-6	16	1
12 Jan 1904	10	+4	10	21
16 Jan 1912	12	+6	12	27
29 Oct 1920	2	+7	2	11
26 Dec 1925	28	+4	27	22
30 Nov 1933	29	+5	29	24
12 Jan 1934	12	+4	12	12
4 Nov 1948	18	+6	18	22
28 Oct 1966	29	+3	29	3
28 Feb 1955	21	+4	21	14
7 July 1973	22	+4	22	23

Pacaya

14.23, -90.36

11 Mar 1961	9	+7	9	11
4 July 1965	6	-1	5	19
19 Oct 1965	9	-3	9	14
9 Dec 1965	1	+7	1	12
3 Jan 1968	19	-3	19	21
2 Feb 1972	4	-1	4	25
18 Feb 1972	20	+2	20	14
15 Oct 1972	23	-2	23	5

Eruption date	Total Vector	North-South	Synodic	Anomalistic
4 Feb 1976	5	0	5	27
18 Feb 1976	18	0	19	13

Fuego

14.29, -90.53

21 Jan 1932	18	-3	18	16
11 Apr 1953	13	+1	13	14
19 Feb 1957	5	+3	5	19
4 Aug 1962	19	-3	19	0
20 Aug 1962	0	+4	1	4
9 Nov 1962	25	-6	25	8
29 Sept 1963	27	-3	27	9
7 Feb 1966	3	-2	2	16
12 Aug 1966	12	+5	12	10
22 Apr 1967	29	+1	29	27
14 Sept 1971	9	-5	10	22
22 Feb 1973	6	+3	5	26
22 Mar 1973	5	+3	4	2
10 Oct 1974	10	-2	10	13
14 Oct 1974	14	+2	14	17
17 Oct 1974	17	+5	17	20
19 Oct 1974	19	+7	19	22
23 Oct 1974	23	-2	23	25
28 May 1975	4	-5	3	24
23 June 1975	18	-3	18	16
3 Mar 1976	12	-5	12	0

Eruption date	Total Vector	North-South	Synodic	Anomalistic
---------------	--------------	-------------	---------	-------------

Acatenango

14.30, -90.53

18 Dec 1924	7	-1	7	6
14 Mar 1925	5	+3	5	11
7 June 1925	0	+6	1	13
26 Aug 1926	3	0	3	17
13 Nov 1972	22	-2	22	6
5 Dec 1972	15	+7	15	1
30 Dec 1972	10	+4	10	13

Santa Maria

14.45, -91.33

24 Oct 1902	7	-2	8	17
27 Oct 1902	10	+2	11	20
30 Oct 1902	13	+4	14	23
1 Nov 1902	15	+6	16	25
6 Nov 1902	21	-4	21	2
29 June 1922	20	-2	20	14
1 July 1922	22	0	22	16
4 Sept 1922	29	-4	28	25
15 Oct 1922	11	-1	11	7
16 Feb 1923	17	-3	16	25
5 May 1923	6	-4	6	21
10 May 1923	10	+1	10	25
13 May 1923	13	+4	13	0
23 May 1923	23	-1	23	10

Eruption date	Total Vector	North-South	Synodic	Anomalistic
15 July 1923	16	-1	16	10
11 Aug 1923	14	-5	14	9
2 Sept 1923	7	+3	7	2
11 Sept 1923	16	-1	16	10
15 Oct 1923	21	+4	21	16
28 Oct 1923	4	+4	4	3
16 Jan 1924	25	+3	25	25
3 Feb 1924	14	-7	18	14
6 Feb 1924	17	-3	16	21
29 June 1924	14	+6	15	1
4 Aug 1924	20	-1	20	8
16 Nov 1924	6	-5	5	2
7 Dec 1924	26	+3	26	24
21 Dec 1924	10	+2	10	2
14 May 1928	10	-1	10	10
20 Feb 1929	28	+7	27	15
15 Mar 1929	20	+3	20	12
13 July 1929	22	0	22	22
27 Sept 1929	9	-5	9	14
2 Nov 1929	16	+4	16	2
10 Nov 1929	24	-2	24	3
13 Nov 1929	27	+1	27	6
26 Nov 1929	10	+1	10	19
28 Nov 1929	12	+3	12	21
16 Dec 1929	0	+6	0	13
28 Aug 1930	20	+1	20	20

Eruption date	Total Vector	North-South	Synodic	Anomalistic
28 Mar 1931	25	-4	25	10
5 Oct 1931	9	-4	9	10
17 Oct 1931	22	-6	21	22
4 Nov 1931	9	0	9	11
22 May 1932	2	-6	2	19
24 May 1932	4	-4	4	21
5 Jan 1933	5	-2	5	5
14 Dec 1934	24	-1	24	18
26 Dec 1934	6	-2	6	1
14 Apr 1956	19	+7	18	12
9 June 1968	29	+4	29	14
14 June 1968	5	-2	5	23
15 Aug 1968	7	+2	8	27
2 Sept 1968	26	+7	26	17
12 Jan 1969	9	+2	9	10
26 Jan 1969	23	+3	23	25
3 Feb 1969	1	-3	1	5
2 Mar 1969	29	-3	29	5
11 July 1969	12	+6	12	26
26 July 1969	28	+6	28	13
25 Sept 1969	0	0	0	19
7 Nov 1969	13	+2	13	6
19 Apr 1973	3	+6	5	12

Colima

19.25, -103.40

30 Dec 1965	24	0	24	5
-------------	----	---	----	---

Eruption date	Total Vector	North-South	Synodic	Anomalistic
30 Jan 1973	12	+7	12	2
1 Dec 1975	14	+6	13	17
28 Jan 1976	29	+7	28	22
9 Mar 1976	24	0	24	5

APPENDIX II

Irazu

Date	Character of eruption	Rating	Source
27 Dec 1917	Explosion	2	Mooser, et al.
30 Jan 1918	Explosion	1	Mooser, et al.
25 July 1918	Explosion	1	Mooser, et al.
9 Aug 1962	Explosion, fumerole	1	ICAITI, p. 3-5
2 Apr 1963	Explosion, ash	1	ICAITI, p. 3-5
17 Apr 1963	Explosion, ash	1	ICAITI, p. 3-5
9 June 1963	Explosion, ash	1	ICAITI, p. 3-5
25 June 1963	Explosion, ash	1	ICAITI, p. 3-5
3 Sept 1963	Explosion, ash	1	ICAITI, p. 3-5
14 Jan 1964	Explosion, ash	1	ICAITI, p. 3-5
18 Feb 1964	Explosion, ash	1	ICAITI, p. 3-5
23 Mar 1964	Explosion, ash	1	ICAITI, p. 3-5
14 Apr 1964	Explosion, ash	1	ICAITI, p. 3-5
6 June 1964	Explosion, ash	1	ICAITI, p. 3-5
2 July 1964	Explosion, ash	1	ICAITI, p. 3-5
7 July 1964	Explosion, ash	1	ICAITI, p. 3-5

Poas

25 Jan 1910	Phreatic expl. mud erupt.	1	Mooser, et al.
30 May 1914	Phreatic expl. mud erupt.	2	Mooser, et al.

Rating - 1 Very important
 2 Important
 3 Moderate
 4 Weak

BVE - Bulletin of Volcanic Eruptions
 ICAITI - Instituto Centroamericano de
 Investigacion y Tecnologia
 Industrial

CSLP - Center for Short-Lived Phenomena
 SEAN - Scientific Event Alert Network

Date	Character of eruption	Rating	Source
8 Oct 1914	Phreatic expl. mud erupt.	2	Mooser, et al.
25 Dec 1957	Steam eruption	2	ICAITI, p. 1
23 May 1963	Explosion, ash	3	BVE, #3
2 July 1963	Explosion, ash	2	BVE, #4
25 Dec 1964	Ash	2	BVE, #5
1 Jan 1967	Explosion	2	BVE, #7
3 May 1969	Vapor eruption	2	CSLP, 44-69
3 June 1969	Explosion, smoke	3-4	CSLP, 44-69
9 Feb 1972	Phreatic explosion	3	BVE, #12
14 Feb 1972	Phreatic explosion	3	BVE, #12
27 Feb 1972	Phreatic explosion	3	BVE, #12
29 May 1972	Phreatic explosion	3	BVE, #12
9 June 1972	Phreatic explosion	3	BVE, #12
18 June 1972	Phreatic explosion	3	BVE, #12
21 June 1972	Phreatic explosion	3	BVE, #12
27 Oct 1972	Phreatic explosion	3	BVE, #12
9 Nov 1972	Phreatic explosion	3	BVE, #12
25 Jan 1973	Explosion	2	BVE, #13
28 Jan 1973	Explosion	2	BVE, #13
9 Feb 1973	Explosion	2	BVE, #13
3 Apr 1973	Explosion, ash	2	BVE, #13
11 Apr 1973	Explosion, ash	2	BVE, #13
8 Sept 1973	Explosion, ash	2	BVE, #13

Arenal

29 July 1968	Nuee ardente	1	CSLP, 20-68
1 Aug 1968	Ash cloud, vapor	1	CSLP, 20-68

Date	Character of eruption	Rating	Source
4 Aug 1968	Ash cloud, vapor	1	CSLP, 20-68
10 Aug 1968	Fumerole	1	CSLP, 20-68
14 Sept 1968	Explosion	1	CSLP, 20-68
19 Sept 1968	Explosion	1	CSLP, 20-68
1 Oct 1968	Lava flows	1	CSLP, 20-68
3 May 1969	Ash eruption	2	CSLP, 20-68
17 June 1975	Lava avalanche	1	SEAN, v.1 #13

Vieja

15 Sept 1966	Explosion, phreatic	2	BVE, #7
29 Nov 1966	Explosion, destruction land	2	BVE, #7
10 June 1967	Explosion, destruction land	1	BVE, #7
22 Apr 1969	Ash explosion	2	CSLP, 41-69

Conception

2 Apr 1957	Explosion	2	Mooser, et al.
28 Nov 1961	Ash eruption	3	BVE, #2
9 May 1963	Ash eruption	3	BVE, #3
24 Dec 1973	Ash eruption	3	BVE, #13
12 Jan 1974	Ash eruption	3	BVE, #13
5 Apr 1977	Explosion	3	Stoiber, pers.
29 Apr 1977	Explosion	2	Stoiber, pers.

Masaya

27 Feb 1927	Explosion, solfatara	1	Mooser, et al.
13 July 1946	Explosion	2	ICAITI, p. 9
10 Oct 1965	Explosion, lava	2	ICAITI, p. 9

Momotombo

Date	Character of eruption	Rating	Source
16 Jan 1905	Explosion, lava	2	Mooser, et al.

Las Pilas

23 Oct 1952	Explosion	2	Mooser, et al.
29 Oct 1954	Explosion	2	Mooser, et al.

Telica

16 Jan 1965	Ash, gas emission	3	ICAITI, p. 7
24 Jan 1965	Ash eruption	3	ICAITI, p. 7
11 Feb 1969	Ash, steam	3	CSLP, 13-69
3 Nov 1976	Ash	3	SEAN, v.1 #14

Cerro Negro

12 June 1947	Explosion, lava, death	1	Mooser, et al.
21 Nov 1950	Explosion, lava	2	Mooser, et al.
17 Dec 1950	Explosion, lava	2	Mooser, et al.
4 Sept 1957	Bombs, lava	1	ICAITI, p. 8
24 Sept 1957	Explosion, bombs, lava	1	ICAITI, p. 8
25 Oct 1961	Explosion, lava	1	BVE, #2
27 Mar 1962	Explosion, ash, lava	1	BVE, #2
24 Oct 1968	Explosion	1	BVE, #8
6 Dec 1968	Explosion	1	BVE, #8
21 Dec 1969	Eruption	2	BVE, #8
3 Feb 1971	Bombs, ash	1	BVE, #11
6 Feb 1971	Bombs, ash	1	BVE, #11
9 Feb 1971	Explosion, bombs, ash	1	BVE, #11

San Cristobal

Date	Character of eruption	Rating	Source
3 May 1971	Explosion, (ash and steam)	2	BVE, #11
30 Nov 1971	Sulfur gas emission	2	BVE, #11
9 Mar 1976	Explosion	2	Hazlett
16 Mar 1976	Explosion	2	Hazlett
29 Aug 1976	Explosion	2	Hazlett

San Miguel

10 Dec 1919	Explosion	2	Mooser, et al.
14 Aug 1920	Explosion	2	Mooser, et al.
23 Oct 1964	Explosion, rock fall	2	ICAITI, p. 13.
22 Feb 1966	Fumerolic activity	3	Stoiber, Rose, 1970
5 Jan 1966	Fumerolic activity	3	Stoiber, Rose, 1970
30 Mar 1970	Explosion	3	BVE, #10
2 Dec 1976	Ash, sulfur	3	SEAN, v. #15

San Salvador

6 June 1917	Boccas became active after earthquake	2	Mooser, et al.
-------------	---------------------------------------	---	----------------

Izalco

10 May 1902	Explosion	2	Mooser, et al.
30 Dec 1902	Explosion	2	Mooser, et al.
12 Jan 1904	Explosion	2	Mooser, et al.
16 Jan 1912	Explosion	2	Mooser, et al.
29 Oct 1920	Explosion	2	Mooser, et al.
26 Dec 1925	Explosion	1	Mooser, et al.

Date	Character of eruption	Rating	Source
30 Nov 1933	Explosion	2	Mooser, et al.
12 Jan 1934	Explosion, lava	2	Mooser, et al.
4 Nov 1948	Explosion	2	Mooser, et al.
28 Feb 1955	Nuee ardente, explosion	1	Mooser, et al.
28 Oct 1966	Explosion, lava	2	Stoiber, et al. 1975

Pacaya

11 Mar 1961	Explosion	1	ICAITI, p. 29
4 July 1965	Explosion, gas	2	ICAITI, p. 31
19 Oct 1965	Explosion, gas, bombs	1	ICAITI, p. 31
9 Dec 1968	Explosion, lava, bombs	1	ICAITI, p. 32
3 Jan 1968	Explosion	2	BVE, #8
2 Feb 1972	Explosion	2	BVE, #12
18 Feb 1972	Explosion	2	BVE, #12
15 Oct 1972	Explosion	2	BVE, #12
4 Feb 1976	Steam, ash	3	SEAN, v.1 #5
18 Feb 1976	Explosion	3	SEAN, v.1 #5

Fuego

21 Jan 1932	Explosion	2	Mooser, et al.
11 Apr 1953	Large noise, extrusion lava	1	Mooser, et al.
19 Feb 1957	Explosion, nuee ardente	1	Mooser, et al.
4 Aug 1962	Explosion, lava, ash	1	ICAITI, p. 22
9 Nov 1962	Explosion, ash	1	BVE, #3
29 Sept 1963	Explosion	1	BVE, #4
7 Feb 1963	Explosion	3	BVE, #7
12 Aug 1966	Ash cloud	1	Hazlett

Date	Character of eruption	Rating	Source
22 Apr 1967	Ash eruption	1	Hazlett
14 Sept 1971	Ash eruption, ash flow	1	CSLP, 85-71
22 Feb 1973	Eruption, ash flow	2	CSLP, 24-73
22 Mar 1973	Ash cloud	3	Hazlett
10 Oct 1974	Explosion	1	CSLP, 134-74
14 Oct 1974	Explosion	1	CSLP, 134-74
17 Oct 1974	Explosion	1	CSLP, 134-74
19 Oct 1974	Explosion	2	CSLP, 134-74
23 Oct 1974	Explosion	1	CSLP, 134-74
28 May 1975	Ash cloud	4	CSLP, 134-74
23 June 1975	Ash eruption	3	CSLP, 134-74
3 Mar 1976	Steam cloud	4	SEAN, v.2 #3

Acatenango

18 Dec 1924	Explosion	2	Mooser, et al.
14 Mar 1925	Bombs, ash	2	Mooser, et al.
7 June 1925	Explosion	3	Mooser, et al.
26 Aug 1926	Vapor, ash eruption	3	Mooser, at al.
13 Nov 1972	Radial fissure eruption	2	BVE, #12
5 Dec 1972	Explosion	3	BVE, #12
30 Dec 1972	Fumerole	3	BVE, #12

Santa Maria (and Santiaguito) from Rose, 1970

Date	Description	Source
24-26 Oct 1902	Initial and strongest phase of 1902 eruption-produced the bulk of 5.5KM ³ of pyroclastic debris	Sapper, 1913

Date	Description	Source
27 Oct 1902	Large ash eruption; 4 PM	Sapper, 1904
30 Oct 1902	2 large ash eruptions, 11 AM 2:30 PM	Sapper, 1904
1 Nov 1902	Large ash eruption, 11:30-12AM	Sapper, 1904
6-7 Nov 1902	Large ash eruption	Sapper, 1904
29 June 1922	Small ash falls, Costa Cuca- Tapachula	Von Tuerckheim 1922 (N.Y. Times, July 3, 1922) Sapper, 1925
4-8 Sept. 1922	Spectacular glowing rock falls, south side	Sapper, 1925
15 Oct 1922	Ash fall at Las Majadas	Sapper, 1925
16-22 Feb 1923	Rumblings heard in Quezaltenango ash falls at San Felipe, Retalhuleu	Sapper, 1925
5-6 May 1923	Compact, steam clouds observed from Quezaltenango	Sapper, 1925
10 May 1923	Compact, steam clouds observed from Quezaltenango	Sapper, 1925
13 May 1923	Largest ash eruption since June 1922 15 mm of ash at Xepach	Sapper, 1925
23-25 May 1923	"Incredible rolling noises", hot muddy water in R. Tambor	Sapper, 1925
15 July 1923	Small nuee ardentes	Sapper, 1925
11-13 Aug 1923	Small ash falls at coastal points more small nuees	Sapper, 1925
2 Sept 1923	Strong steam clouds observed from Quezaltenango	Sapper, 1925
11 Sept 1923	Strong steam clouds observed from Quezaltenango	Sapper, 1925
15 Oct 1923	$\frac{1}{2}$ mm ash fall at Santa Maria de Jesus	Sapper, 1925
28 Oct 1923	Small nuee ardentes	Sapper, 1925
16 Jan 1924	Minor quakes and ash falls, strong sulfur smell at Quezaltenango	Sapper, 1926
3 Feb 1924	Ash falls E and SE of crater	Sapper, 1925

Date	Description	Source
6 Feb 1924	Strong white eruption cloud above crater; observed from Quezaltenango	Sapper, 1925
29-30 June 1924	Ash falls at many fincas along Boca Costa	Alvarado, 1936
4 Aug 1924	Bright incandescence at night ash clouds	Sapper, 1925
16 Nov 1924	Glowing cloud	Sapper, 1925
7-30 Dec 1924	Fine white ash fall at Xepach thick steam clouds persist to height of Santa Maria	Sapper, 1925
21 Dec 1924	Small glowing cloud	Sapper, 1925
14 May 1928	Large ash eruption; 4-7 mm of ash fall in coastal slope	Termer, 1929
20-28 Feb 1929	Large ash eruptions; strong quakes Ash falls as far as Tapachula	Deger, 1931, N.Y. Times, Feb 22,24,27, 1929 Alvarado, 1936
15 Mar 1929	Ash eruption	Kaiser, 1929
13 July 1929	Ash eruption, glowing cloud	Sapper and Termer, 1930a
27-29 Sept 1929	Ash eruptions, strong glow of dome at night	Sapper and Termer, 1930a
2-5 Nov 1929	Series of large, glowing clouds, many killed; ash eruptions accompany	Sapper and Termer, 1930b Deger, 1931
10 Nov 1929	Glowing cloud	N.Y. Times, Nov 11, 1929
13 Nov 1929	Ash eruptions	Sapper and Termer, 1930b
26 Nov 1929	High cauliflower ash cloud light quakes	Sapper and Termer, 1930b
28 Nov 1929	Ash, tremors	N.Y. Times, Nov 29, 1929
16 Dec 1929	Large steam-ash cloud; glowing cloud, 5 PM Large landslide, 10AM	Sapper and Termer, 1930b

Date	Description	Source
28 Aug 1930	Ash eruption; ash fall as fall as V. Tacana; glowing cloud to Tambor Valley	Termer, 1930
28 Mar 1931	Glowing cloud to Rio Tambor, 7:45 AM	Termer, 1934
5 Oct 1931	Glowing cloud in Rio Tambor Valley	Termer, 1934
17 Oct 1931	Glowing cloud in Rio Tambor Valley	Termer, 1934
4 Nov 1931	Steam and ash eruption	Termer, 1934
22 May 1932	Strong activity (glowing cloud?) follows strong quake	Termer, 1934
24-27 May 1932	Series of glowing clouds	Termer, 1934
5 Jan 1933	Steam and ash eruption; blocks thrown to 100 M. height	Termer, 1934
14 Dec 1934	Ash eruption, 6:30 AM, ash fall at San Francisco Zapotitlan Quake follows eruption, 8:30AM	El Imparcial, 14-15 Dec 1936
26 Dec 1934	Ash fall at San Francisco Zapotitlan	Von Tuerckheim, 1935
14 Apr 1956	Large ash eruption ash to Quezaltenango, El Palmar, San Felipe and W. El Salvador	Meyer-Abich, 1956
9-14 June 1968	Several large ash eruptions; ash fall and SO ₂ odor at Llano del Pinal, 7 km NE	<u>Prensa Libre</u> June 14, 1968
14 July 1968	Blocks as large as 20x20x40 cm are thrown a distance of 500 m laterally from the vent	Field notes
15 Aug 1968	White ash fall at Quezaltenango, 12 km NE; 3:30 PM	Field notes
2 Sept 1968	Tremors precede large black ash and bomb explosion. Noise heard in Quezaltenango. Bombs 40x40x40 cm as far as 1 km from vent; 9:50 AM	Field notes
12-19 Jan 1969	Series of large ash eruptions. ash falls at Quezaltenango on Jan 19, 8 AM	<u>Prensa Libre</u> Jan 20, 1969

Date	Description	Source
26 Jan 1969	Very strong SO ₂ odor at Quezaltenango	Field notes
3 Feb 1969	Very strong SO ₂ odor at Quezaltenango 11:15 PM	Field notes
16 Feb 1969	Very high ash cloud; strong SO ₂ odor reaches Quezaltenango; 8:45 AM	Field notes
2 Mar 1969	SO ₂ odor at Quezaltenango; 6:10 AM	Field notes
30 Mar 1969	Loud noise heard at Llano del Pinal; 4 AM	Field notes
11 July 1969	Loud explosion heard at Llano del Pinal; 11 PM. Bombs as large as 1x1x3 m thrown 500 m laterally from the vent	Field notes
26 July 1969	Ash and bombs erupted with strong high black and white ash cloud. Tremors felt in Llano del Pinal; Ash cloud visible in Quezaltenango 8:30 PM	Field notes
25 Sept 1969	Ash fall at Quezaltenango, SO ₂ smell ash column visible 1:30 PM, bombs and tremors felt at Buena Vista	<u>Prensa Libre</u> Sept 26,27 1969
7 Nov 1969	Strong eruption cloud observed and SO ₂ smell noticed at Llano del Pinal	Field notes
19 Apr 1973	Phreatic explosion, lava	BVE, #13
17 Sept 1973	Phreatic explosion, lava	BVE, #13
Colima		
30 Dec 1965	Explosion, lava dome extruded	2 BVE, #7
30 Jan 1973	Ash, bombs	2 BVE, #13
1 Dec 1975	Explosion, lava dome	2 SEAN, v.1 #3
28 Jan 1976	Lava flow	3 SEAN, v.1 #4

Date	Character of eruption	Rating	Source
9 Mar 1976	Lava	4	SEAN, v.1 #6

REFERENCES

- Allen, M.W., 1936, The lunar triggering effect of earthquakes in southern California: Bull. Seismol. Soc. Amer., v. 26, p. 147-157.
- Annual Report of the World Volcanic Eruptions, 1973-1976: Bull. Volcanologique, v. 37,38,39.
- Bulletin of Volcanic Eruptions, 1976: Inter. Assoc. of Volcanology and Chemistry of the Earth's Interior, I.U.G.G.
- Hamilton, W.L., 1973, Tidal cycles of volcanic eruptions: fortnightly to 19 year periods: Jour. Geophys. Res., v. 78, p. 3363-3375.
- Hazlett, R.W., 1977, Geology and hazards of the San Cristobal volcanic complex, Nicaragua: unpub. M.S. thesis, Dartmouth College, Hanover, N.H., 212 p.
- Instituto Centroamericano de Investigacion y Tecnologia Industrial (ICIATI), 1966, Report of Active Volcanoes in Central America during 1957 to 1965, 35 p.
- Klein, F.W., 1976, Earthquake swarms and the semidiurnal solid earth tide: Geophys. J.R. astr. Soc., v. 45, p. 245-295.
- Knopoff, L., 1964, Earth tides as a triggering mechanism for earthquakes: Bull. Seismol. Soc. Amer., v. 54, p. 1865-1870.
- Longman, I.M., 1959, Formulas for computing the tidal accelerations due to the moon and the sun: Jour. Geophys. Res., v. 64, p. 2351-2355.
- Mauk, F.J., and Johnson, M.J.S., 1973, On the triggering of volcanic eruptions by earth tides: Jour. Geophys. Res., v. 78, p. 3356-3362.
- _____ and Kienle, J., 1973, Microearthquakes at St. Augustine Volcano, Alaska, triggered by earth tides: Science, v. 182, p. 386-389.
- Mooser, F., Meyer-Abich, H., and McBirney, H.P., 1958, Catalog of Active Volcanoes of the World, Including Solfatara Fields: Inter. Volcanological Assoc.
- Morgan, W.J., Stoner, J.O., and Dicke, R.H., 1961, Periodicity of Earthquakes and the Invariance of the gravitational constant: Jour. Geophys. Res., v. 66, p. 3831-3843.
- Pollack, H.N., 1964, Longman tidal formulas: resolution of horizontal components: Jour. Geophys. Res., v. 78, p. 2598.
- Rose, W.I., 1970, Geology of the Santiaguito volcanic dome, Guatemala: unpub. PhD. thesis, Dartmouth College, Hanover, N.H., 254 p.
- Ryall, A., Van Wormer, J.D., and Jones, A.E., 1968, Triggering of micro-earthquakes by earth tides, and other features of the Truckee,

California, earthquake sequence of September, 1966, Bull. Seismol. Soc. Amer., v. 58, p. 215-248.

Scientific Event Alert Network (SEAN), 1975-1977: Smithsonian Institution and Museum of Natural History.

Simpson, J.F., 1967, Earth tides as a triggering mechanism for earthquakes: Earth and Planet. Sci. Lett., v. 2, p. 473-478.

Smithsonian Institution Center for Short-Lived Phenomena, 1969-1971: Annual Reports.

Stoiber, R.E., and Carr, M.J., 1973, Quaternary volcanic and tectonic segmentation of Central America: reprint from Bull. Volcanologique, v. 37, p. 304-325.

_____, and Rose, W.I., Jr., 1970, The geochemistry of Central American volcanic gas condensates: Bull. Geol. Soc. Amer., v. 81, p. 2891-2912.

_____, Lange, I.M., Birnie, R.W., 1975, The cooling of Izalco volcano (El Salvador), 1964-1974: Geol. Jb. 813, p. 193-205.

Tamrazyan, G.P., 1969, Seismicity of Norway in relation to cosmic conditions: Norsk Geologisk Tidsskrift, v. 49, p. 81-86.